ACCOUNTS of chemical research

Article

pubs.acs.org/accounts

Group 9 Organometallic Compounds for Therapeutic and Bioanalytical Applications

Dik-Lung Ma,*[,†] Daniel Shiu-Hin Chan,[†] and Chung-Hang Leung*[,‡]

[†]Department of Chemistry, Hong Kong Baptist University, Kowloon Tong, Hong Kong, China

[‡]State Key Laboratory of Quality Research in Chinese Medicine Institute of Chinese Medical Sciences, University of Macau, Macao SAR, China

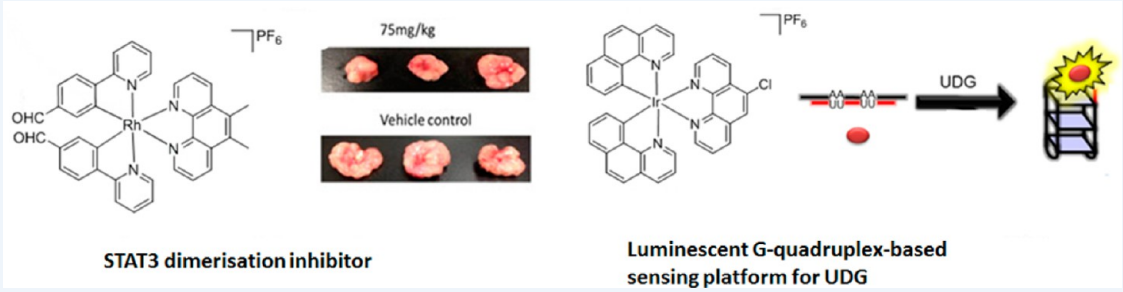

CONSPECTUS: Compared with organic small molecules, metal complexes offer several distinct advantages as therapeutic agents or biomolecular probes. Carbon atoms are typically limited to linear, trigonal planar, or tetrahedral geometries, with a maximum of two enantiomers being formed if four different substituents are attached to a single carbon. In contrast, an octahedral metal center with six different substituents can display up to 30 different stereoisomers. While platinum- and ruthenium-based anticancer agents have attracted significant attention in the realm of inorganic medicinal chemistry over the past few decades, group 9 complexes (i.e., iridium and rhodium) have garnered increased attention in therapeutic and bioanalytical applications due to their adjustable reactivity (from kinetically liable to substitutionally inert), high water solubility, stability to air and moisture, and relative ease of synthesis. In this Account, we describe our efforts in the development of group 9 organometallic compounds of general form $[M(C^{\wedge}N)_2(N^{\wedge}N)]$ (where M = Ir, Rh) as therapeutic agents against distinct biomolecular targets and as luminescent probes for the construction of oligonucleotide-based assays for a diverse range of analytes.

Earlier studies by researchers had focused on organometallic iridium(III) and rhodium(III) half-sandwich complexes that show promising anticancer activity, although their precise mechanisms of action still remain unknown. More recently, kinetically-inert group 9 complexes have arisen as fascinating alternatives to organic small molecules for the specific targeting of enzyme activity. Research in our laboratory has shown that cyclometalated octahedral rhodium(III) complexes were active against Janus kinase 2 (JAK2) or NEDD8-activating enzyme (NAE) activity, or against NO production leading to antivasculogenic activity *in cellulo*. At the same time, recent interest in the development of small molecules as modulators of protein−protein interactions has stimulated our research group to investigate whether kinetically-inert metal complexes could also be used to target protein−protein interfaces relevant to the pathogenesis of certain diseases. We have recently discovered that cyclometalated octahedral iridium(III) and rhodium(III) complexes bearing C^N ligands based on 2-phenylpyridine could function as modulators of protein−protein interactions, such as TNF-α, STAT3, and mTOR. One rhodium(III) complex antagonized STAT3 activity *in vitro* and *in vivo* and displayed potent antitumor activity in a mouse xenograft model of melanoma. Notably, these studies were among the first to demonstrate the direct inhibition of protein−protein interfaces by kinetically-inert group 9 metal complexes. Additionally, we have discovered that group 9 solvato complexes carrying 2-phenylpyridine coligands could function as inhibitors and probes of β-amyloid fibrillogenesis.

Meanwhile, the rich photophysical properties of iridium complexes have made them popular tools for the design of luminescent labels and probes. Luminescent iridium(III) complexes benefit from a high quantum yield, responsive emissive properties, long-lived phosphorescence lifetimes, and large Stokes shift values. Over the past few years, our group has developed a number of kinetically-inert, organometallic iridium(III) complexes bearing various C^N and N^N ligands that are selective for G-quadruplex DNA, which is a DNA secondary structure formed from planar stacks of guanine tetrads stabilized by Hoogsteen hydrogen bonding. These complexes were then employed to develop G-quadruplex-based, label-free luminescence switch-on assays for nucleic acids, enzyme activity, small molecules, and metal ions.

Received: August 21, 2014
Published: November 4, 2014

1. INTRODUCTION

Group 9 (i.e., rhodium and iridium) complexes have recently attracted increasing attention as therapeutic agents.[1−5] Sheldrick[6] and Sadler[7] have extensively investigated cytotoxic iridium(III) "half-sandwich" anticancer complexes of type $[(\eta^5\text{-Cp*})\text{Ir(XY)Z}]^{n+}$ (Figure 1), in which the pentamethylcyclopentadienyl ligand (Cp*) (or its derivatives) not only stabilizes the iridium metal center but also enhances the kinetic lability of the *trans*-monodentate leaving group ligands, thereby activating the complexes toward DNA coordination. In a rapidly emerging subdiscipline, Meggers and co-workers have pioneered the application of kinetically-inert metal complexes (Figure 1) as molecularly targeted inhibitors of enzyme activity, with some of these displaying remarkable affinity and selectivity for their target enzymes despite using only reversible interactions.[8]

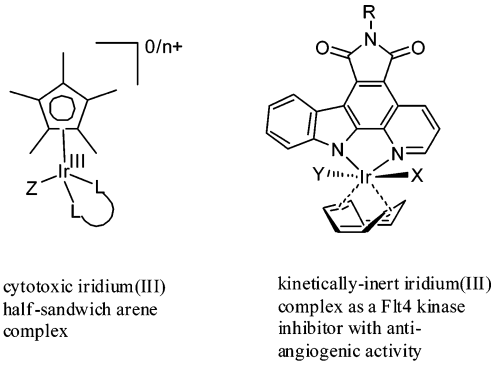

cytotoxic iridium(III) half-sandwich arene complex

kinetically-inert iridium(III) complex as a Flt4 kinase inhibitor with anti-angiogenic activity

Figure 1. General structure of half-sandwich iridium(III) cyclopentadienyl complexes (left) and kinetically-inert iridium(III) pyridocarbazole complexes (right).

Besides therapeutic applications, group 9 complexes have also found use as luminescent probes or labels for biomolecules or metal ions,[9−13] as exemplified by the iridium(III) complexes developed for the detection of Hg^{2+} ions,[14] Cu^{2+} ions,[15] Zn^{2+} ions,[16] or human serum albumin[17] in our laboratory. Compared with organic molecules, transition metal complexes possess unique advantages for biosensing applications, such as (i) high luminescence quantum yield, (ii) sensitivity of their emissive behavior to changes in the local environment, (iii) long phosphorescence lifetime that allows their emission to be distinguished from a fluorescent background by time-resolved luminescence spectroscopy, (iv) large Stokes shift, and (v) modular synthesis that allows the efficient synthesis of analogues for optimization of their properties. The purpose of this Account is to present recent efforts from our laboratory in the application of group 9 organometallic complexes, particularly octahedral iridium(III) or rhodium(III) complexes of general form $[M(C^\wedge N)_2(N^\wedge N)]$, as medicinal or bioanalytical agents.

2. GROUP 9 ORGANOMETALLIC COMPOUNDS FOR THERAPEUTIC APPLICATIONS

2.1. Group 9 Metal Complexes Targeting Enzymes

Janus kinases (JAKs) are intracellular, nonreceptor tyrosine kinases that mediate transduction signals via the JAK/STAT pathway, thereby controlling cell proliferation, differentiation, cell migration, and apoptosis.[18] Our group has identified $[Rh(ppy)_2(CN\text{-}L)_2]OTf$ (**1**, ppy = 2-phenylpyridinato, CN-L_2 = 2-naphthylisocyanide) and $[Rh(bzq)_2(CN\text{-}L)_2]OTf$ (**2**, bzq = benzoquinoline) as metal-based inhibitors of JAK2 (Figure 2).[19] Both complexes inhibited JAK2 activity in a cell-free system and in human erythroleukemia (HEL) cells, which harbor a V617F mutation in JAK2 leading to constitutive kinase activity without affecting total JAK2 expression. Moreover, both complexes displayed cytotoxic activity against HEL cells.

NEDD8-activating enzyme (NAE) plays an important role in the maintenance of protein homeostasis. Our group has identified the rhodium(III) complex $[Rh(ppy)_2(dppz)]OTf$, **3** (dppz = dipyrido[3,2-*a*:2′,3′-*c*]phenazine), as a metal-based inhibitor of NAE.[20] Complex **3** suppressed Ubc12−NEDD8 conjugation both in a cell-free system and in human epithelial colorectal adenocarcinoma (Caco-2) cells, with selectivity over the related SUMO-activating enzyme (SAE) (Figure 3a). Moreover, **3** blocked the degradation of the cullin−RING ubiquitin E3 ligase (CRL) substrates IκBα and $p27^{kip1}$ and repressed tumor necrosis factor-α (TNF-α)-induced NF-κB activation in cells. Molecular modeling analysis of the **3**−NAE−NEDD8 interaction showed that the rhodium(III) center was situated in the central canyon-like groove of NAE, while the dppz moiety contacted the UBA3 subunit of NAE (Figure 3b).

The excess production of nitric oxide (NO) by nitric oxide synthase (iNOS) has been implicated in the pathogenesis of autoimmune or inflammatory processes.[21] Our group has discovered a novel rhodium(III) complex **4** that reduced lipopolysaccharide (LPS)-induced NO production and NF-κB transcriptional activity in RAW 264.7 macrophages (Figure 4).[22] Furthermore, **4** reduced vasculogenic activity in human umbilical vein endothelial cells (HUVECs) at submicromolar concentrations.

2.2. Group 9 Metal Complexes Targeting Protein−Protein Interactions and Protein Aggregation

Protein−protein interactions are ubiquitous in fundamental biological processes such as cell proliferation and differentiation, host−pathogen interactions, and signal transduction pathways.[23] However, targeting protein−protein interactions has historically

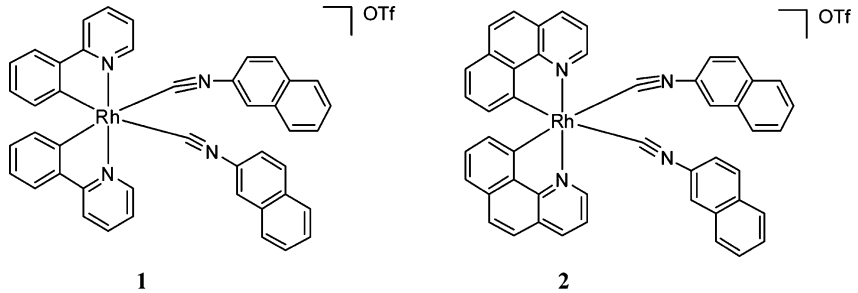

Figure 2. Complexes **1** and **2**.

dx.doi.org/10.1021/ar500310z | *Acc. Chem. Res.* 2014, 47, 3614−3631

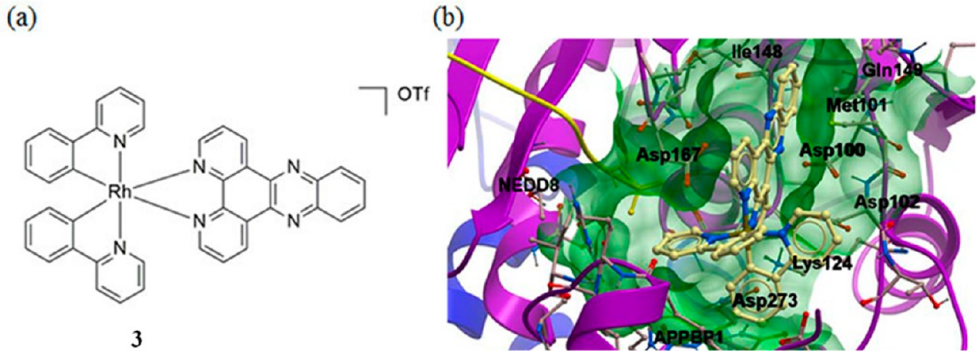

Figure 3. (a) Complex **3** and (b) docking diagram of **3** bound to the NAE heterodimer.[20]

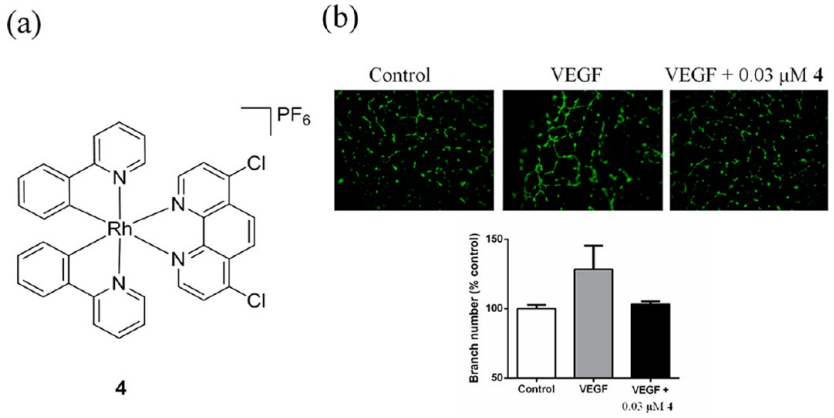

Figure 4. (a) Complex **4** and (b) inhibition of vasculogenic activity by **4** *in cellulo*. Reproduced from ref 22 with permission. Copyright 2014 Elsevier.

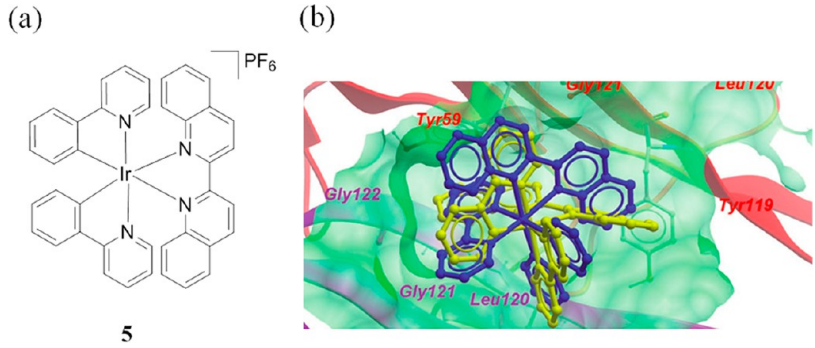

Figure 5. (a) Complex **5** and (b) docking diagram of Δ-**5** (blue) and Λ-**5** (yellow) bound to the TNF-α dimer. Reproduced with permission from ref 25. Copyright 2012 Wiley-VCH.

been considered to be a difficult task due to their typically large sizes (>1500 Å) and featureless interfaces that lack well-defined crevices for recognition by small molecules. In this respect, transition metal complexes possess distinct geometries that can enable the design of unique structural architectures for probing the binding surface of protein−protein interactions. However, few metal-based protein−protein modulators have yet been reported in the literature.

TNF-α is a multifunctional cytokine that regulates an array of biological processes, including apoptosis, cell survival, immunity, and inflammation.[24] Our group has reported the iridium(III) complex **5**, $[Ir(ppy)_2(biq)]PF_6$ (biq = 2,2′-biquinoline), as a metal-based inhibitor of TNF-α activity.[25] Molecular modeling analysis showed that the aromatic biq and ppy ligands of both the Δ- and Λ-enantiomers of **5** were able to contact the β-strands of both subunits of the TNF-α dimer complex (Figure 5), thereby blocking the association of the third TNF-α subunit to form the active trimer complex. In biological assays, **5** inhibited the binding of TNF-α to TNFR-1 *in vitro* and antagonized TNF-α-induced NF-κB transcriptional activity *in cellulo*. This study was one of the first to demonstrate the direct inhibition of a protein−protein interface by a kinetically-inert group 9 metal complex.

The role of signal transducer and activator of transcription 3 (STAT3) in controlling cell progression, cell survival, and differentiation has rendered it an attractive target for anticancer strategies.[26] Recently, our group has discovered the cyclometalated rhodium(III) complex **6** as the first example of a substitutionally inert group 9 organometallic compound that directly targeted the SH2 domain of STAT3 (Figure 6a).[27] After two rounds of screening of an in-house library of rhodium(III) and iridium(III) complexes, **6** was identified as a lead compound that exhibited potent antiproliferative activity against human

dx.doi.org/10.1021/ar500310z | *Acc. Chem. Res.* 2014, 47, 3614−3631

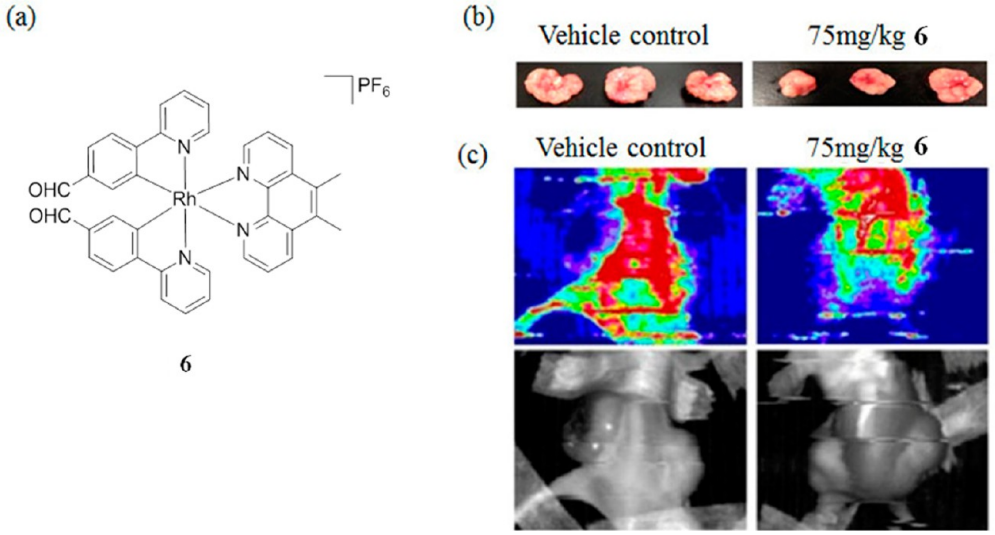

Figure 6. (a) Complex **6**, (b) photographs of dissected tumors, and (c) laser Doppler flowmetry to assess blood flow around the tumor site *in vivo*. Reproduced with permission from ref 27. Copyright 2014 Wiley-VCH.

melanoma cells *in vitro* while being relatively nontoxic toward normal cells. In cellular assays, **6** attenuated STAT3 Y705 phosphorylation, STAT3 dimerization, and STAT3-driven transcriptional activity. Importantly, **6** reduced tumor size and weight in an *in vivo* mouse xenograft model without causing overt toxicity to the mice (Figure 6b). Tumor tissues treated with **6** showed repressed STAT3 phosphorylation and decreased COX-2, iNOS, and VEGF expression. Moreover, **6** reduced blood flow around the periphery of the tumor site *in vivo* (Figure 6c). Finally, unlike previous iridium(III) and rhodium(III) complexes developed by our group, **6** showed no significant effect against mTOR activity or TNF-α binding, indicating the importance of chemical structure in determining the selectivity of these substitutionally inert complexes against protein targets.

The mammalian target of rapamycin (mTOR) is a serine/threonine kinase that is dysregulated in a number of human cancers.[28] Our group has recently identified the rhodium(III) complex **7** (Figure 7) as a metal-based stabilizer of the

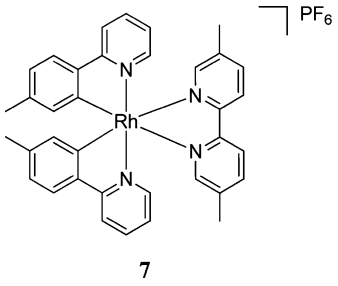

Figure 7. mTOR inhibitor **7**.

mTOR–FKBP12 interaction.[29] From an in-house panel of rhodium(III) complexes, **7** showed the highest ability to attenuate mTOR activity *in vitro* and *in cellulo*, with potency comparable to that of rapamycin. Structure–activity relationship analysis indicated that the 5,5′-dimethyl-2,2′-bipyridine ligand of **7** was important for mTOR inhibitory activity, whereas more bulky or more polar N^N ligands led to reduced activity. Moreover, changing the metal center from rhodium(III) to iridium(III) resulted in decreased activity. This indicates the importance of the rhodium(III) center in providing an optimum arrangement of the coligands in the complex to achieve greater binding affinity for the mTOR or FKBP12 proteins. Interestingly, this is different from certain complexes reported by the group of Meggers, where the ruthenium(III) and osmium(III) congeners showed similar activity against Pim-1, suggesting that the metal ion played a purely structural role.[30]

Our efforts have led to the development of an iridium(III) solvato complex, $[Ir(ppy)_2(solv)_2]^+$, that was applied for luminescent protein staining.[31] The iridium(III) solvato complex $[Ir(ppy)_2(DMSO)_2]^+$ was subsequently utilized by Li and co-workers as a luminescent imaging agent for live cell nuclei.[32] In 2011, our group reported the application of the group 9 solvato complexes $[Rh(ppy)_2(H_2O)_2]OTf$ (**8**) and $[Ir(ppy)_2(H_2O)_2]OTf$ (**9**) (Figure 8) as inhibitors of amyloid fibrillogenesis and as luminescent probes for β-amyloid peptide.[33] These complexes contained aromatic C^N ligands to interact with the hydrophobic residues around the N-terminal domain of the Aβ peptide, as well as solvato coligands to allow coordinative bond formation with histidine residues in the protein, thereby preventing the aggregation of the Aβ peptide into neurotoxic Aβ fibrils. Notably, the ability of **8** to inhibit Aβ fibrillogenesis was superior to that of previous metal-based inhibitors reported. Moreover, the phosphorescence response of **9** to aggregated Aβ fibrils was nearly three times higher than that for an equal mass concentration of monomeric Aβ peptides (Figure 8c). This suggests that these complexes could be used to differentiate between the monomeric and fibrillar forms of Aβ or to monitor Aβ fibrillogenesis.

3. GROUP 9 METAL COMPLEXES FOR BIOANALYTICAL APPLICATIONS

3.1. Principles and Advantages of Label-Free G-Quadruplex-Based Luminescent Assays

The G-quadruplex is a noncanonical DNA secondary structure that possesses a diverse array of structural topologies depending on the number and length of the guanine tracts, the nature of the intervening loops, and the character of the metal ion in solution.[34,35] The extensive structural heterogeneity of G-quadruplex motifs has rendered them as versatile signal-transducing elements in DNA-based sensing applications.[36]

dx.doi.org/10.1021/ar500310z | Acc. Chem. Res. 2014, 47, 3614–3631

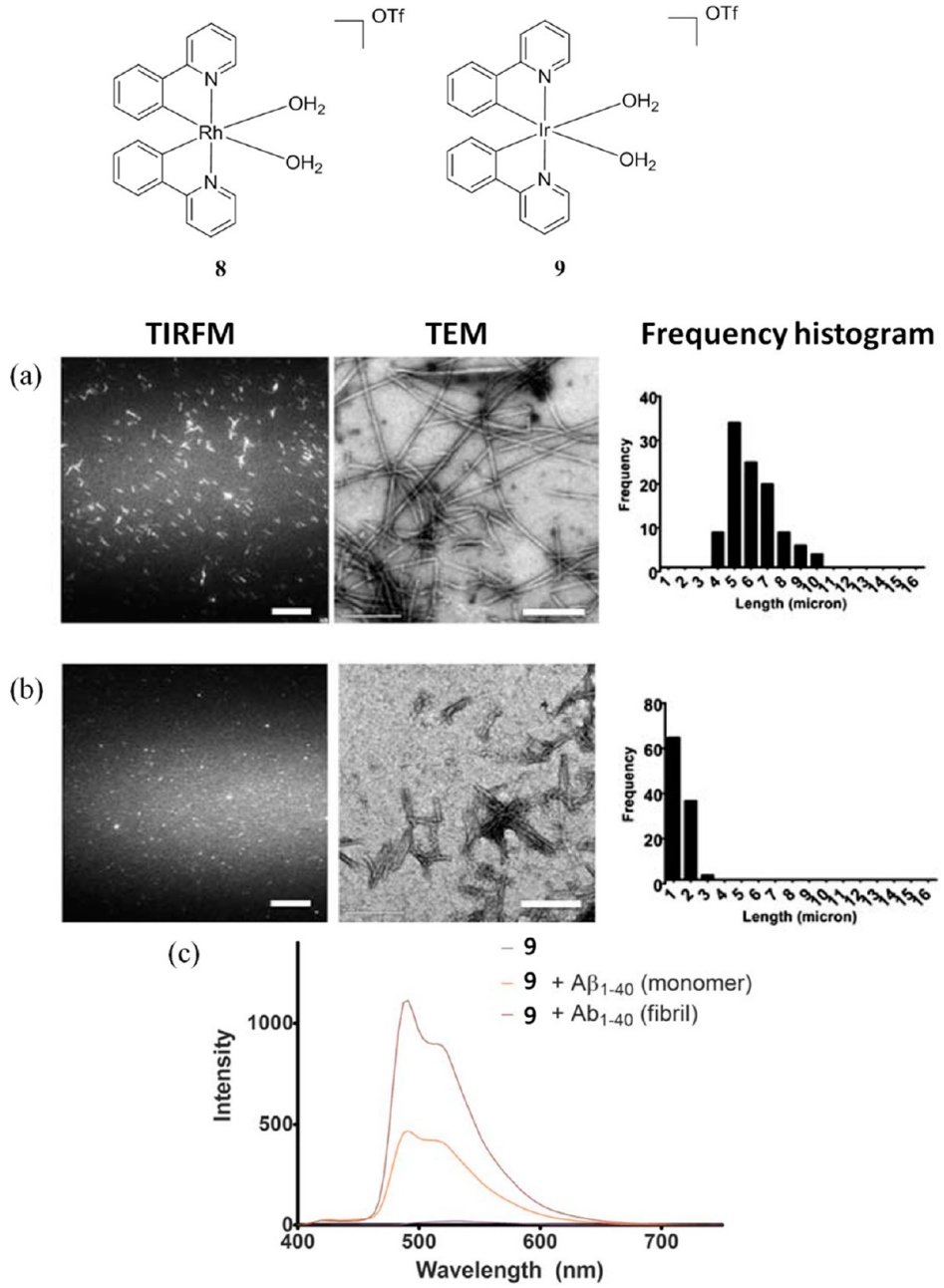

Figure 8. Total internal reflection fluorescence microscopy (TIRFM) fluorescence images (left), transmission electron microscopy (TEM) images (center), and the frequency histogram (right) of Aβ growth in the (a) absence and (b) presence of **8**, and (c) emission spectra of **9** in the absence and presence of Aβ peptide monomers and fibrils. Reproduced from ref 33 with permission. Copyright 2011 The Royal Society of Chemistry.

Early DNA-based sensors typically employed labeled oligonucleotides that are covalently conjugated to donor/acceptor or fluorophore/quencher pairs. However, fluorescent labeling can be relatively costly and laborious and may adversely impact the behavior of the functional oligonucleotide.[37] In the label-free approach, luminescent probes are not covalently conjugated to the nucleic acid backbone but instead interact noncovalently with DNA via intercalation, groove-binding, end-stacking, or electrostatic interactions. Both organic dyes and metal complexes have found use for the development of label-free G-quadruplex-based detection platforms.[36,38] Compared with using labeled oligonucleotides, the label-free approach is more time and cost-effective because expensive and tedious prelabeling or immobilization steps are avoided. Additionally, the labeling of an oligonucleotide with a fluorophore may disrupt the interaction between the oligonucleotide and its cognate target. Notably, the label-free assays developed by our group have, in many cases, achieved detection limits comparable to those using labeled oligonucleotides. However, one drawback of the label-free approach is the lack of true multiplex capability, since the proximity of different luminophores with their respective oligonucleotides cannot be precisely controlled.

Our group has developed luminescent iridium(III) complexes that are selective for G-quadruplex DNA over single-stranded DNA (ssDNA) or double-stranded DNA (dsDNA), with some even showing selectivity for specific G-quadruplex conformations. We then employed these luminescent iridium(III) complexes for the construction of G-quadruplex-based switch-on

dx.doi.org/10.1021/ar500310z | Acc. Chem. Res. 2014, 47, 3614−3631

assays for a range of biologically and environmentally important analytes, such as metal ions, small molecules, or enzyme activity. In the context of metal ion detection, the chief advantages of our G-quadruplex-based luminescent assays compared with instrumental methods such as inductively coupled plasma mass spectrometry (ICP-MS) and atomic absorption/emission spectroscopy (AAS/AES) is that they are simple and rapid to use and are amenable to real-time analysis or in-field studies with the aid of portable spectrophotomers. However, luminescent oligonucleotide-based assays tend to have lower sensitivity compared with those instrumental methods. In terms of protein or enzyme activity detection, the advantages of the label-free luminescent assays are more significant. Conventional assays for protein or enzyme activity based on enzyme-linked immunosorbent assay (ELISA) or gel electrophoresis tend to be tedious, discontinuous, and multistep, and may require stringent protocols to control radiographic exposure. Hence, the G-quadruplex-based luminescent assays developed by our group potentially represent a significant upgrade over existing methods for the detection of various enzyme activities.

3.2. Early Studies Using $[Ir(ppy)_2(biq)_2]^+$

Early in our independent research careers, the well-known "light-switch" ruthenium(II) complex, $[Ru(phen)_2(dppz)]^{2+}$ (phen = 1,10-phenanthroline), was utilized to develop a switch-on assay for transcription factor activity.[39] Inspired by this result, we envisioned that the aromatic coligands of $[Ir(ppy)_2(biq)_2]^+$ would be able to form effective π-stacking interactions with the terminal G-tetrad of the G-quadruplex structure. Encouragingly, we found that the addition of the G-quadruplex Pu22 (5′-$GAG_3TG_4AG_3TG_4A_2G$-3′) resulted in a 4-fold increase in the luminescence intensity of complex **5** (Figure 9). By comparison,

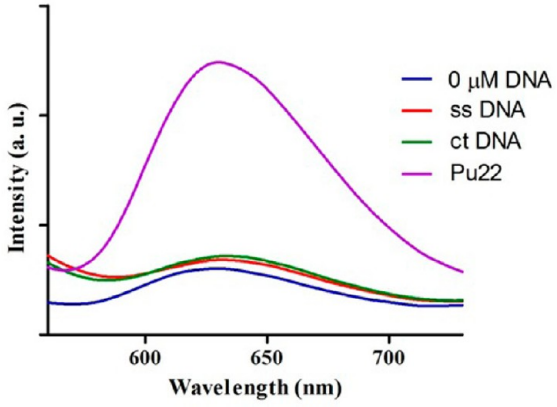

Figure 9. Luminescence response of complex **5** in the presence of various DNAs. Reproduced from ref 41 with permission. Copyright 2012 The Royal Society of Chemistry.

in the presence of calf thymus (ct) DNA or ssDNA, no significant luminescence enhancement was observed.

We therefore investigated the suitability of complex **5** as a G-quadruplex-specific probe for the construction of an oligonucleotide-based assay for Pb^{2+} ions.[40] Upon binding to Pb^{2+} ions, the oligonucleotide PS2.M (5′-$GTG_3TAG_3CG_3T_2G_2$-3′) adopts a G-quadruplex conformation, which greatly enhances the luminescence emission of **5** (Figure 10). The assay could detect down to 600 pM of Pb^{2+} ions and was selective for Pb^{2+} over 10-fold excess of other metal ions such as K^+, Ag^+, Na^+, Ni^{2+}, Cr^{3+}, Hg^{2+}, Zn^{2+}, Mg^{2+}, Ca^{2+}, and Ba^{2+} ions.

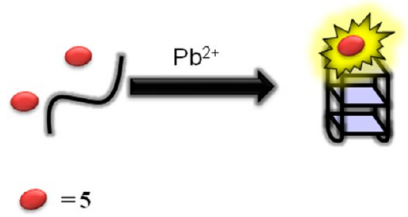

Figure 10. G-quadruplex-based assay for Pb^{2+} ions.

We also investigated the application of complex **5** to construct a split G-quadruplex-based detection platform for gene deletion (Figure 11).[41] A split G-quadruplex is generated from the

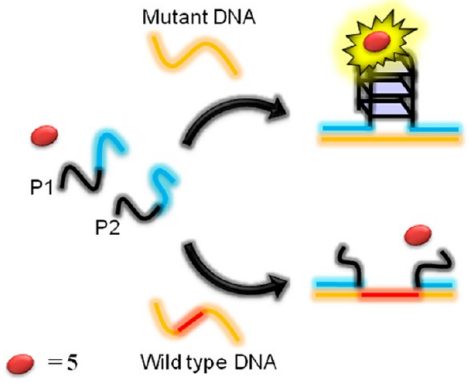

Figure 11. Split G-quadruplex-based detection strategy for gene deletion.

intermolecular association of two short oligonucleotide sequences, which, being of shorter length, are significantly less expensive than intramolecular G-quadruplex-forming sequences. In the presence of the shorter mutant DNA sequence (5′-$CTCAT_4C_2ATACAT_2A_3GATAGTCAT$-3′) but not the longer wild-type sequence (5′-$CTCAT_4C_2ATACAGTCAGTATCA_2T_2CTG_2A_2GA_2T_3C_2AGACAT_2A_3GATAGTCAT$-3′), the two G-quadruplex-forming sequences (5′-$ATGACTATCT_3A_2TG_3TAG_3$-3′ and 5′-$G_3T_2G_3CGTAG_2A_4TGAG$-3′) are brought into closer proximity, promoting the formation of the split G-quadruplex and producing a significant switch-on luminescence response. This method was also capable of differentiating single-mismatched DNA sequences with a detection limit of 50 nM. A different iridium(III) complex was later used to develop an RNA detection assay using a similar approach.[42]

3.3. Testing Analogues of Iridium(III) Complexes

Based on the success of complex **5** as a G-quadruplex-specific probe,[40,41,43] we were interested to investigate analogues of **5** that might also show G-quadruplex-selective "switch-on" behavior, in order to develop sensing platforms for different types of targets.[44−46] In one study, the luminescent iridium(III) complex $[Ir(phq)_2(2,9\text{-dpphen})]PF_6$, **10** (phq = 2-phenylquinoline, 2,9-dpphen = 2,9-diphenyl-1,10-phenanthroline; Figure 12a), was also found to be G-quadruplex-selective, since it displayed a 4-fold emission enhancement with the PS2.M G-quadruplex (Figure 12b), and was used to construct a G-quadruplex-based luminescent assay for biothiols. In this assay, the addition of biothiols such as cysteine or glutathione can effectively sequester Hg^{2+} ions, liberating the **10**−G-quadruplex ensemble from the quenching effect of Hg^{2+} and restoring the emission of **10** (Figure 12c). Significantly, the

dx.doi.org/10.1021/ar500310z | Acc. Chem. Res. 2014, 47, 3614−3631

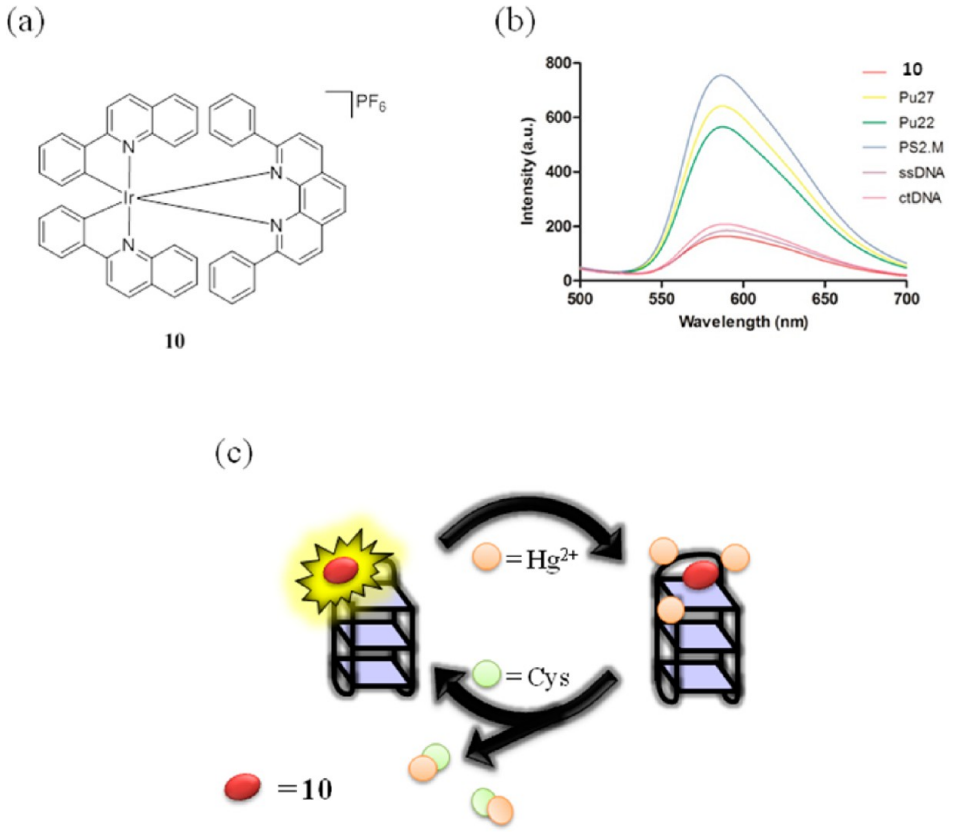

Figure 12. (a) Complex **10**, (b) luminescence response of **10** in the presence of various DNAs, and (c) G-quadruplex-based assay for the detection of biothiols. Reproduced from ref 47 with permission. Copyright 2012 The Royal Society of Chemistry.

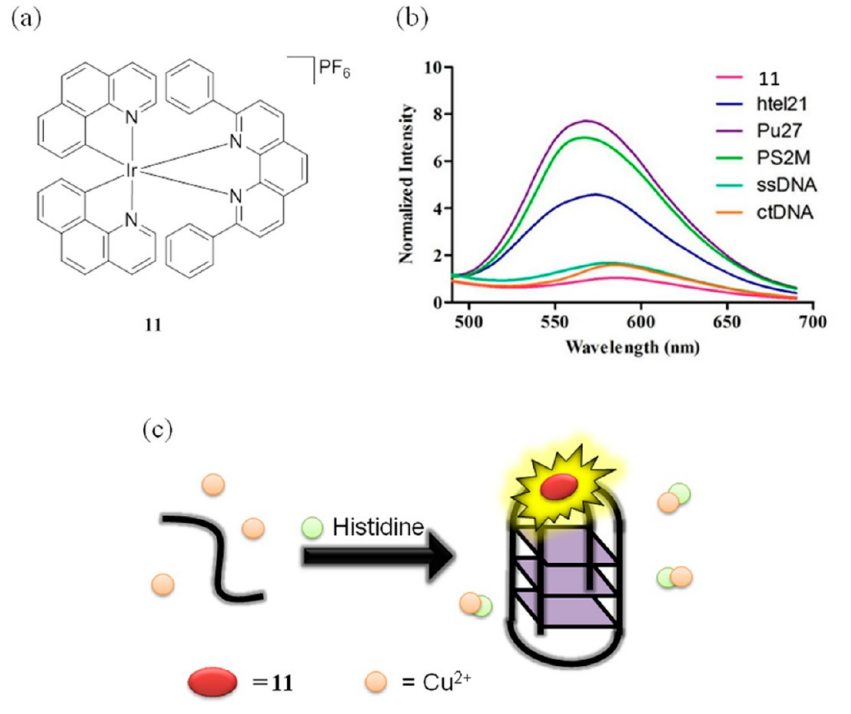

Figure 13. (a) Complex **11**, (b) luminescence response of **11** in the presence of various DNAs, and (c) G-quadruplex-based assay for histidine. Reproduced from ref 48 with permission. Copyright 2013 Elsevier.

assay exhibited a tunable range for the detection of biothiols that could be controlled by varying the concentration of Hg^{2+} ions.[47]

Like **10**, the iridium(III) complex $[Ir(bzq)_2(2,9\text{-dpphen})]PF_6$ **11**, which exhibited a 5-fold luminescent response to the Pu27 G-quadruplex, also carries the 2,9-dpphen N^N ligand, though it

dx.doi.org/10.1021/ar500310z | Acc. Chem. Res. 2014, 47, 3614−3631

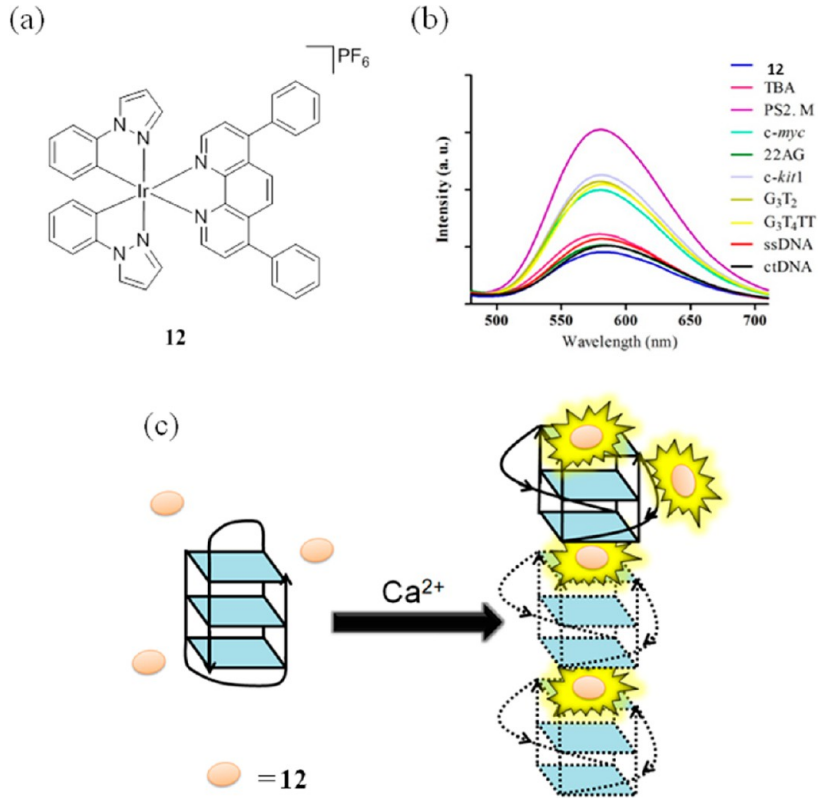

Figure 14. (a) Complex **12**, (b) luminescence response of **12** in the presence of various DNAs, and (c) G-quadruplex-based assay for Ca^{2+} ions. Reproduced from ref 49 with permission. Copyright 2013 Elsevier.

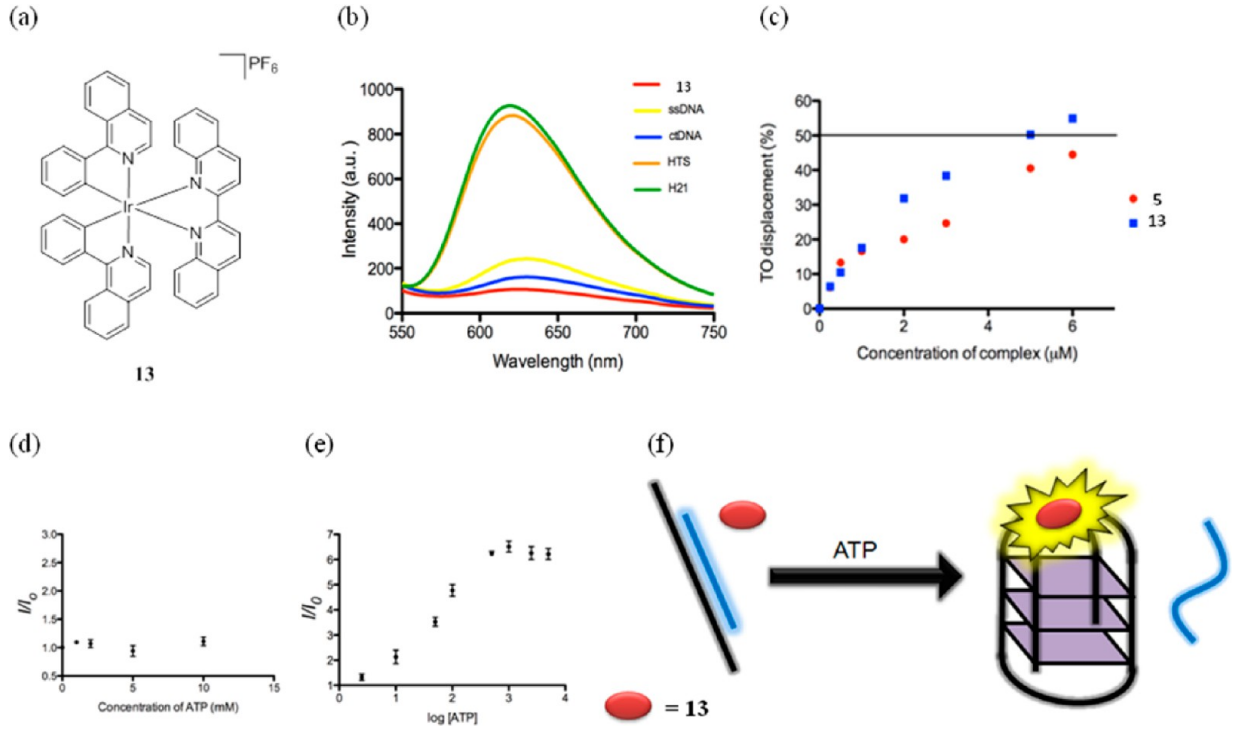

Figure 15. (a) Complex **13**, (b) luminescence response of **13** in the presence of various DNAs, (c) G4-FID titration curves of the ATP G-quadruplex, emission enhancement of the (d) **5**/duplex and (e) **13**/duplex systems in response to ATP, and (f) G-quadruplex-based assay for ATP.[50]

contains a different C^N ligand. In the histidine assay, the initial luminescence of the Pu27 (5′-$TG_4AG_3TG_4AG_3TG_4A_2G_2$-3′)/**11** ensemble is effectively quenched by Cu^{2+} ions due to the Cu^{2+}-mediated unfolding of the G-quadruplex motif (Figure 13).[48] The addition of histidine sequesters Cu^{2+} ions from the ensemble, thereby restoring the luminescence of the system. The assay could detect down to 1 μM of histidine and also exhibited more than a 4-fold stronger luminescence response for histidine than for other

dx.doi.org/10.1021/ar500310z | Acc. Chem. Res. 2014, 47, 3614−3631

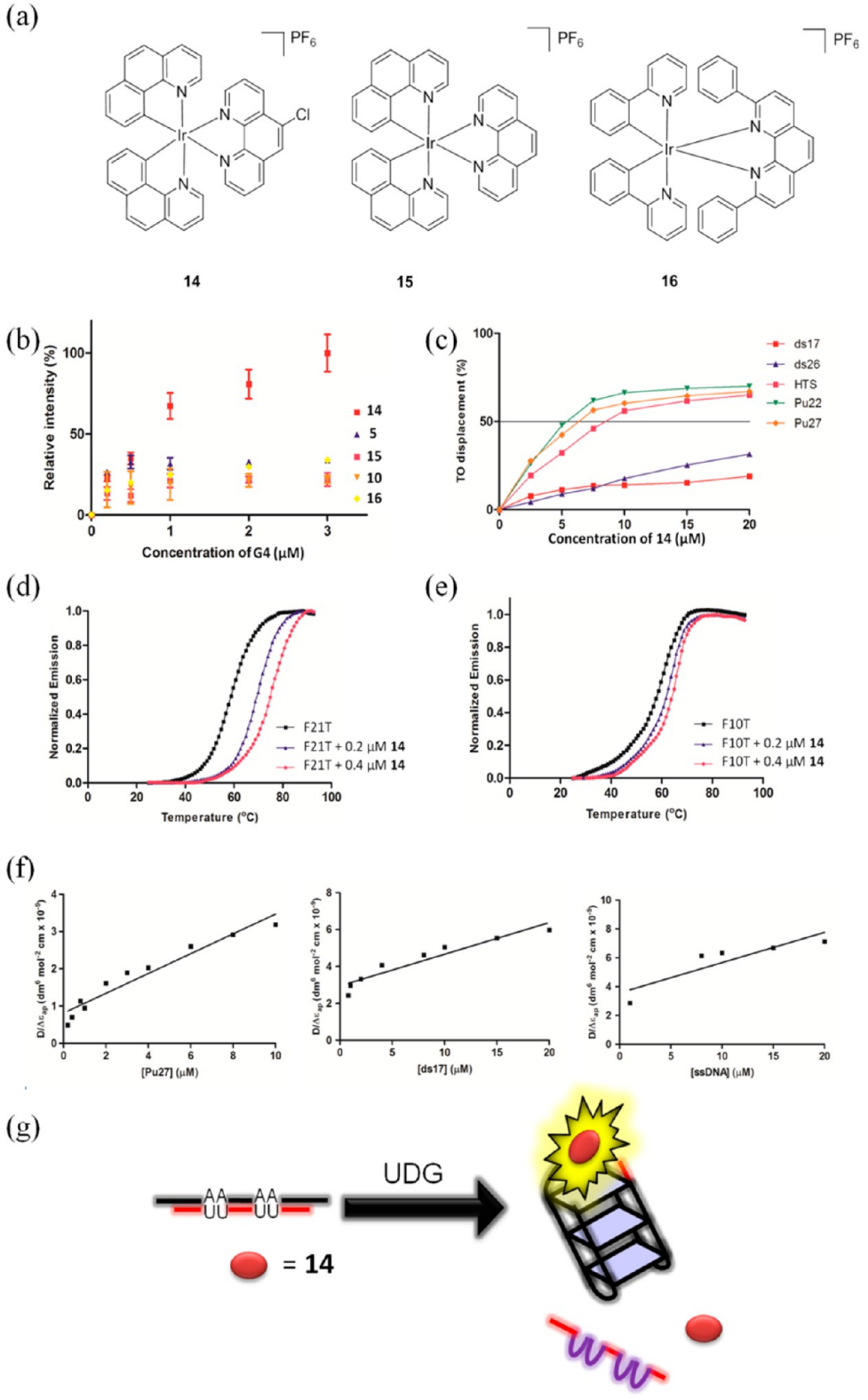

Figure 16. (a) Complexes **14**–**16**, (b) luminescence response of complexes to the G4 G-quadruplex, (c) G4-FID titration curves of DNA duplexes (ds17 and ds26) and G-quadruplexes (Pu22, Pu27, and HTS) with **14**, (d, e) melting profiles showing selectivity of **14**, (f) plot of $D/\Delta\varepsilon_{ap}$ vs concentration of DNA, and (g) G-quadruplex-based assay for UDG. Reproduced from ref 51 with permission. Copyright 2013 The Royal Society of Chemistry.

common amino acids, as well as the thiols cysteine, homocysteine, and GSH with the use of the cysteine-masking agent *N*-ethylmaleimide. Future work could also study the influence of reducing agents such as ascorbate on the performance of this assay.

Changing the 2,9-dpphen ligand of **11** into its regioisomer bathophenanthroline (4,7-dpphen) while replacing the bzq C^N ligands with phenylpyrazole (ppyr) moieties generated complex $[Ir(ppyr)_2(4,7\text{-dpphen})]PF_6$, **12** (Figure 14), which was capable

dx.doi.org/10.1021/ar500310z | *Acc. Chem. Res.* 2014, 47, 3614–3631

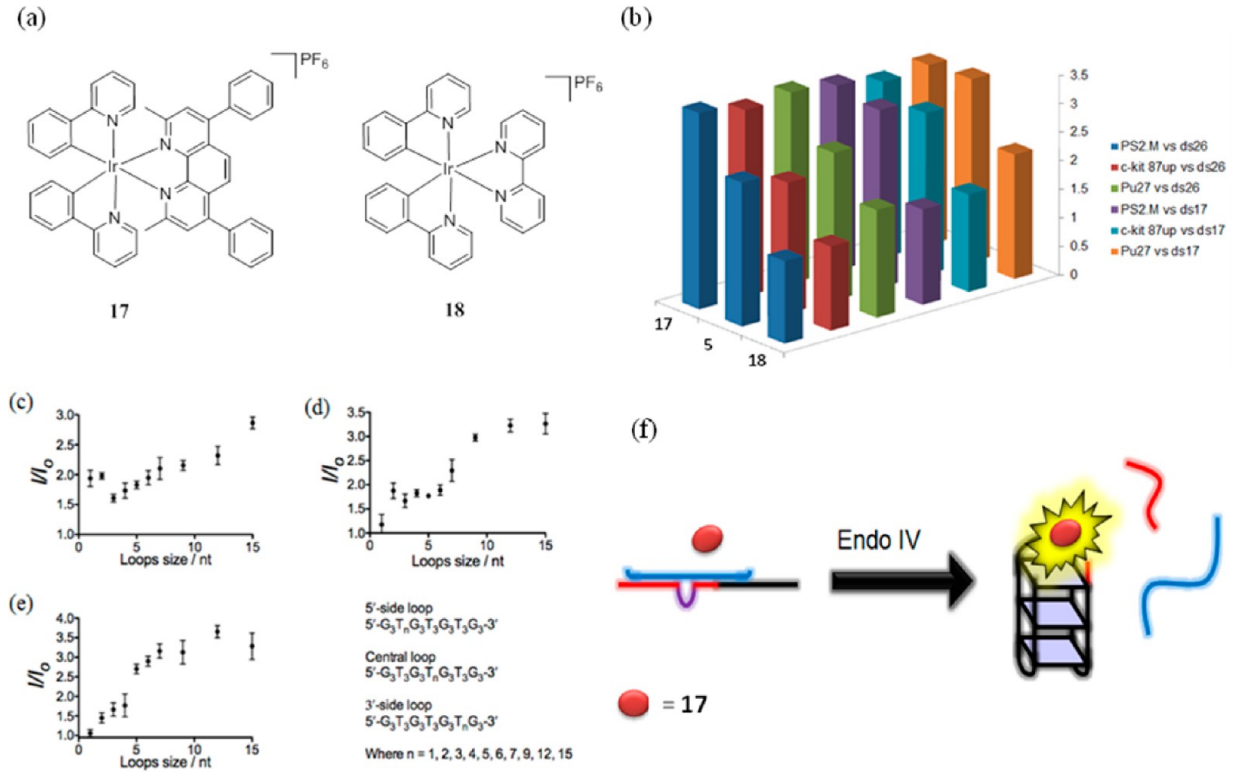

Figure 17. (a) Complexes **17** and **18**, (b) luminescence enhancement selectivity ratio of **5**, **17**, and **18** for G-quadruplex DNA over dsDNA, luminescence enhancement of **18** as a function of loop size for a (c) 5′-side loop, (d) central loop, and (e) 3′-side loop, and (f) G-quadruplex-based assay for Endo IV. Adapted with permission from ref 52. Copyright 2013 American Chemical Society.

of discriminating parallel G-quadruplexes over antiparallel G-quadruplexes.[49] Complex **12** interacted strongly with *c-myc* (5′-$T_2GAG_3TG_2GTAG_3TG_3TA_3$-3′), *c-kit1* (5′-$AG_3AG_3CG$-$CTG_3AG_2AG_3$-3′), PS2.M, G_3T_4TT (5′-$G_3T_4G_3TG_3TG_3$-3′), and G_3T_2 (5′-$G_3T_2G_3T_2G_3T_2G_3$-3) DNA (2.0−3.7-fold luminescent enhancement), which are known to adopt parallel G-quadruplex conformations in the presence of K^+ ions, but not with the antiparallel G-quadruplexes TBA (5′-$G_2T_2G_2TGT$-$G_2T_2G_2$-3′) and 22AG (5′-$AG_3T_2AG_3T_2AG_3T_2AG_3$-3′) (1.1−1.3-fold luminescent enhancement). In the Ca^{2+} detection assay, the addition of Ca^{2+} ions transforms an antiparallel G-quadruplex (5′-$G_4T_4G_4$-3′) into a parallel G-quadruplex conformation, which greatly enhances the luminescence of **12**. This method could detect down to 10 nM Ca^{2+} ions and was selective for Ca^{2+} over a panel of other metal ions (K^+, Mg^{2+}, Ni^{2+}, Hg^{2+}, Pb^{2+}, Cd^{2+}, Zn^{2+}, Cu^{2+}, Li^+, and Ba^{2+}).

3.4. Investigations into G-Quadruplex Selectivity

During our investigation to develop an aptamer-based assay for ATP detection, we were puzzled to observe that complex **5** showed only weak affinity for the ATP aptamer G-quadruplex ensemble. Instead, the iridium(III) complex $[Ir(piq)_2(biq)]PF_6$, **13** (piq =1-phenylisoquinoline), which differs from **5** only in the nature of its C^N ligand, showed a much greater affinity for the ATP aptamer G-quadruplex (Figure 15). Complex **13** also showed a strong luminescent enhancement (8-fold) in the presence of the HTS (5′-$AG_3(T_2AG_3)_3$-3) or H21 (5′-$T_2AG_3T_2AG_3T_2AG_3$-T_2AG_3-3′) G-quadruplex. We reason that the larger C^N ligands of **13** allowed it to form superior end-stacking interactions with the terminal face of the G-quartet. In the ATP-detection assay, the ATP aptamer (5′-$A_2C_2TG_4GAGTAT_2GCG_2AG_2A_2G_2T$-3′) is initially hybridized with its complementary sequence (5′-AC_2T_2-$C_2TC_2GCA_2TACTC_5AG_2T_2$-3′).[50] The duplex-to-quadruplex conversion triggered by ATP could be detected by **13** (but not **5**) with a switch-on luminescence response (Figure 15). This study highlights the important connection between the structure of the iridium(III) complexes and their ability to recognize specific G-quadruplex motifs.

As our research group became more experienced, additional experiments were performed to investigate the relationship between the structure of the iridium(III) complexes and their G-quadruplex selectivity. In one study, we investigated the interaction of $[Ir(bzq)_2(5\text{-Clphen})]PF_6$, **14** (5-Clphen = 5-chloro-1,10-phenanthroline), and other complexes toward a G-quadruplex sequence with a very long loop (G4, 5′-$G_3TAG_3A_3T_2CT_2A_2GTGCG_3T_2G_3$-3′).[51] In emission titration experiments, **14** showed the highest luminescence enhancement (6-fold) toward this long-loop G4 G-quadruplex, whereas the nonhalogenated congener **15** showed a much weaker luminescence response. This result suggests that the chloride group in **14** may play an important role in governing the interaction between **14** and the G-quadruplex. Moreover, the G-quadruplex selectivity of **14** was confirmed by fluorescence resonance energy transfer (FRET) melting assays, G-quadruplex fluorescent intercalator displacement (G4-FID) assays, and UV−vis titration. In the uracil-DNA glycosylase (UDG) assay, UDG splices uracil from the uracil-containing strand of a DNA duplex substrate (5′-$G_3TAG_3A_3T_2CT_2A_2GTGCG_3T_2G_3$-3′ and 5′-$CGCACU_2A_2GA_2U_2TC$-3′), releasing the quadruplex-forming strand that is subsequently recognized by **14** (Figure 16).

We also investigated the effect of the size of N^N ligand of the iridium(III) complexes on their G-quadruplex selectivity. We found that $[Ir(ppy)_2(bcp)]PF_6$, **17** (bcp = 2,9-dimethyl-4,7-diphenyl-1,10-phenanthroline), which exhibited a maximum luminescent enhancement of 3.5-fold with the PS2.M

dx.doi.org/10.1021/ar500310z | Acc. Chem. Res. 2014, 47, 3614−3631

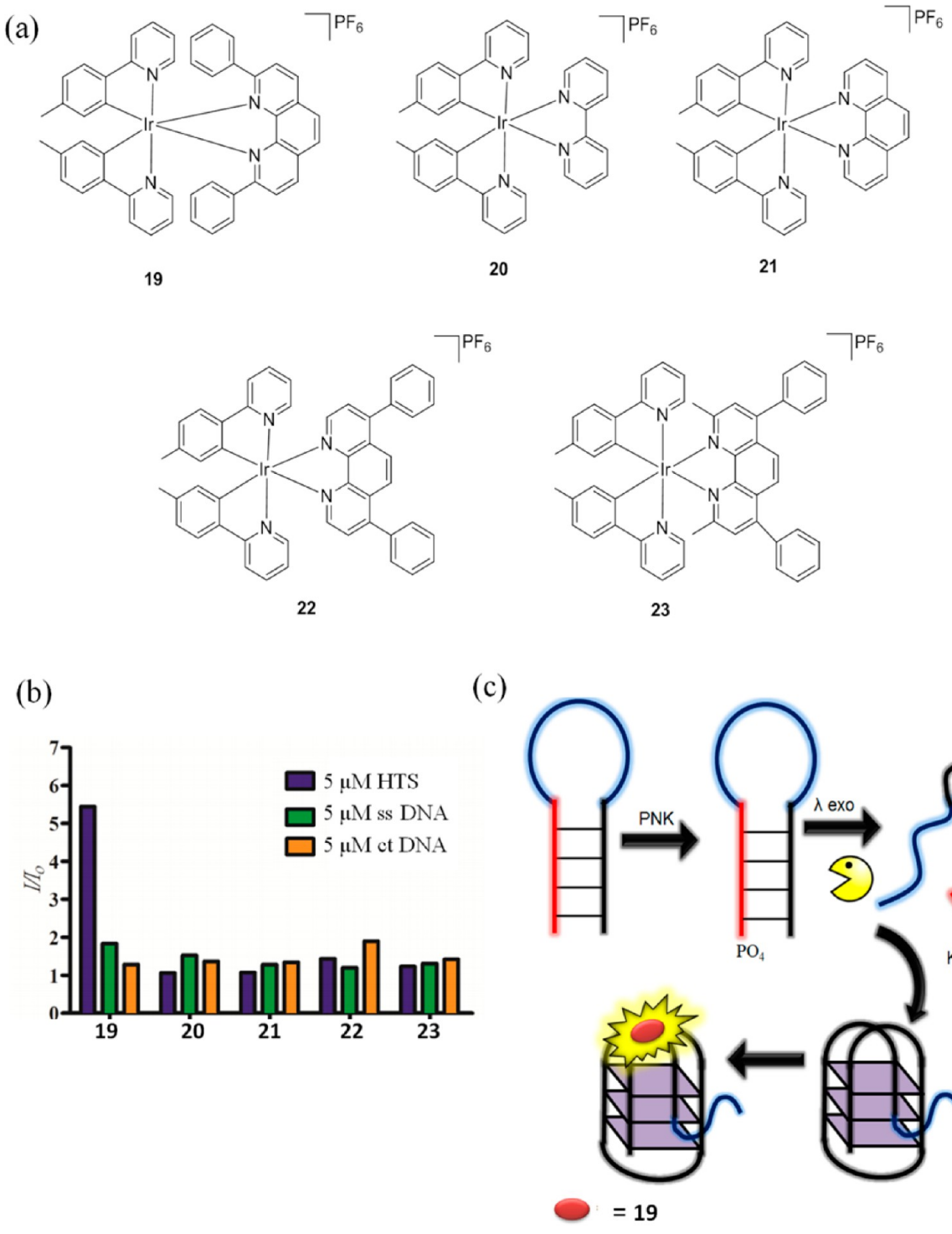

Figure 18. (a) Complexes **19**–**23**, (b) luminescence response of **19**–**23** in the presence of various DNAs, and (c) G-quadruplex-based assay for PNK. Reproduced from ref 53 with permission. Copyright 2014 The Royal Society of Chemistry.

G-quadruplex, showed superior G-quadruplex discriminating ability compared with **5** and **18**, which bear the smaller biq or 2,2′-bipyridine N^N ligands, respectively (Figure 17). This suggests that the size of the N^N ligands is also an important determinant of G-quadruplex-binding selectivity. We further showed that the luminescence intensity of complex **17** generally increased with greater loop size of the G-quadruplex motif, regardless of the location of the loop. We then devised an oligonucleotide-based assay for the detection of apurinic/apyrimidinic (AP) endonuclease activity using **17**.[52] We designed an AP site-containing DNA oligonucleotide (5′-TATCTGCAC*AGTG$_3$TAG$_3$CG$_3$T$_2$G$_2$-3′) that also contains a G-quadruplex-forming sequence at the 3′-terminus and hybridized this with a partially complementary DNA strand (5′-TATCTGCACUAGTG$_3$TAG$_3$CG$_3$T$_2$G$_2$-3′). Cleavage of the AP site in the duplex substrate by endonuclease IV (Endo IV) results in the release of the G-quadruplex-forming fragment that is subsequently recognized by **17**.

dx.doi.org/10.1021/ar500310z | Acc. Chem. Res. 2014, 47, 3614−3631

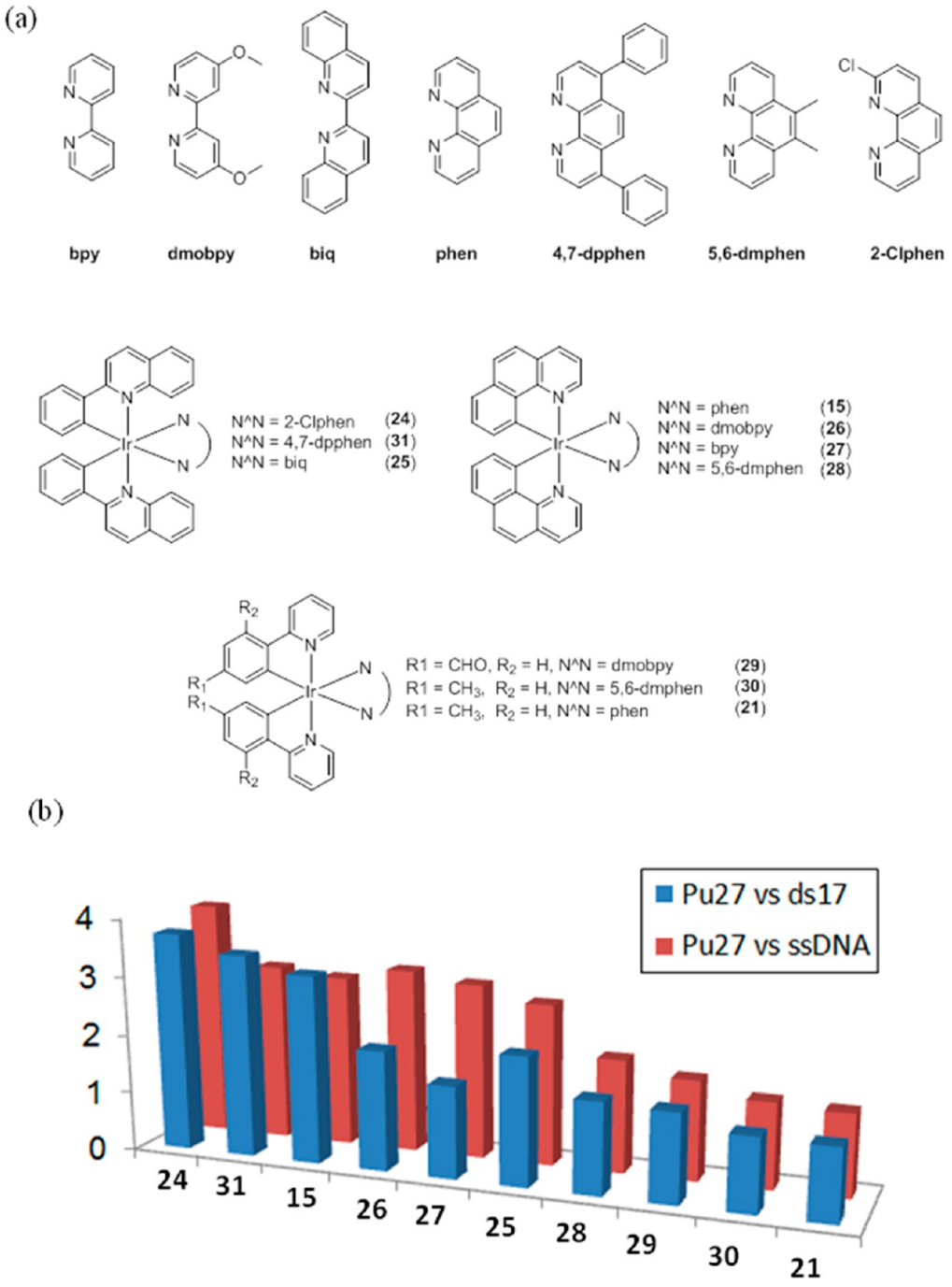

Figure 19. (a) Various iridium(III) complexes and (b) luminescence enhancement selectivity ratio of complexes for G-quadruplex over dsDNA. Reproduced from ref 54 with permission. Copyright 2014 The Royal Society of Chemistry.

3.5. Exploring Larger Libraries of Iridium(III) Complexes

Equipped with a more extensive arsenal of biophysical techniques, as well as larger numbers of iridium(III) complexes at hand, our group began to screen larger libraries of iridium(III) complexes for sensing applications. The advantage of screening a larger number of complexes is that it increases the likelihood of identifying an iridium(III) complex that binds with high affinity and selectivity for a particular G-quadruplex structure. In an early study of this kind, we initially examined the ability of complexes **19**–**23**, which all contained 2-(*p*-tolyl)pyridine (ptpy) C^N ligands, to interact with different forms of DNA by emission titration.[53] The complex $[Ir(ptpy)_2(2,9\text{-dpphen})]PF_6$, **19** (Figure 18), displayed a *ca.* 5.5-fold enhanced luminescence in the presence of the HTS G-quadruplex, while only slight luminescence changes were observed in the presence of ssDNA and ctDNA. This result indicates that **19** was able to discriminate G-quadruplex from duplex or ssDNA. On the other hand, **20**–**23** were found to be nonselective for G-quadruplex. The N^N ligands of **20** and **21** might be too small to form effective end-stacking interactions with the terminal G-quartets, while the pendant phenyl groups of the N^N ligands of **22** and **23** may be in an inappropriate orientation to interact effectively with the G-quadruplex motif. To further validate the suitability of **19** as a G-quadruplex-selective probe, we employed UV/vis absorption titration and G4-FID assays to evaluate the binding affinity and

dx.doi.org/10.1021/ar500310z | *Acc. Chem. Res.* 2014, 47, 3614−3631

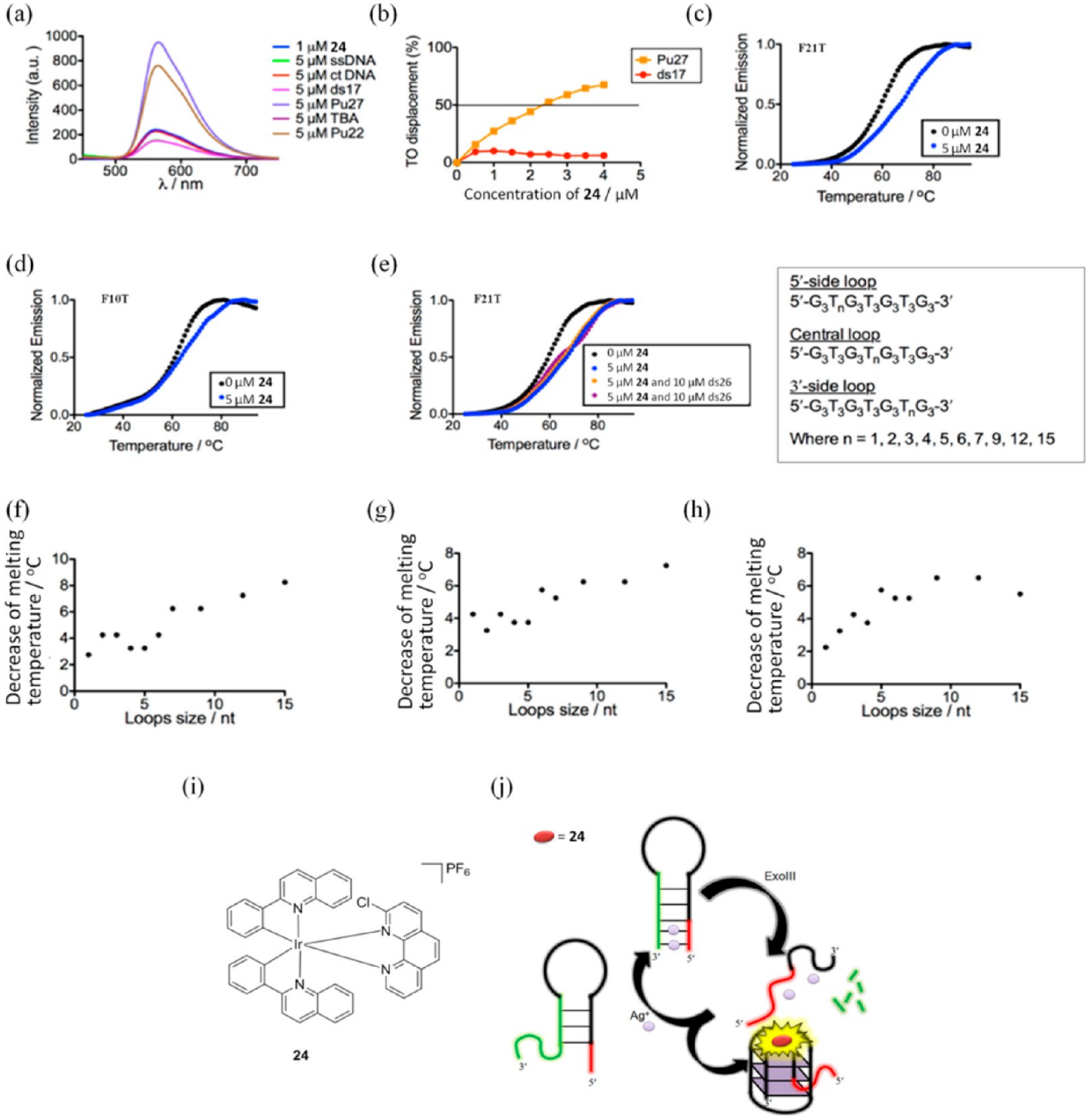

Figure 20. (a) Emission spectrum of complex **24** in the presence of various DNAs, (b) G4-FID titration curves of DNA duplex ds17 or G-quadruplex Pu27, (c–e) melting profiles showing selectivity of **24**, competitive FRET-melting assay for **24** in the presence of G-quadruplexes with different loop lengths as the competitor where the decrease of melting temperature is shown as a function of loop size for a (f) 5′-side loop, (g) central loop, and (h) 3′-side loop, (i) complex **24**, and (j) G-quadruplex-based ExoIII-assisted assay for Ag^+ ions. Reproduced from ref 54 with permission. Copyright 2014 The Royal Society of Chemistry.

selectivity of **19** for G-quadruplex. The differential selectivity of **20**–**23** toward the G-quadruplex motif may be due to differences in the nature of the N^N ligand, with **19** containing the 2,9-dpphen ligand being more able to interact effectively with G-quadruplex structures through groove/loop binding or end-stacking interactions. In the PNK activity assay, 5′-phosphorylation of a hairpin substrate (5′-$(C_3TA_2)_3C_3TA_2TAG_2A_2GACAG_3$ $(T_2AG_3)_3$-3′) by T4 PNK allows cleavage of the 5′-strand by λ exo, and the 3′-guanine-rich sequence is released and folds into a G-quadruplex structure, which is recognized by **19**. The system exhibited a sensitivity of 0.05 U/mL for PNK and was also applied for the screening of potential T4 PNK inhibitors.

Very recently, our group has developed an exonuclease III (ExoIII)-assisted assay for Ag^+ ions using the G-quadruplex-selective iridium(III) complex **24**.[54] Ten complexes (Figure 19) were screened for their ability to selectively distinguish G-quadruplex from dsDNA and ssDNA, of which **24** emerged as a top candidate. Further experiments using emission titration, G4-FID, and FRET-melting assays also confirmed **24** to be a G-quadruplex-selective probe (Figure 20). Intriguingly, complex **24** showed a strong luminescence response (*ca.* 4-fold) to the Pu27 and Pu22 G-quadruplexes but not to the TBA G-quadruplex. The TBA G-quadruplex has been previously shown to accommodate planar aromatic ligands but not ribbon-like molecules,[55] suggesting that **24** may bind outside

dx.doi.org/10.1021/ar500310z | *Acc. Chem. Res.* 2014, 47, 3614–3631

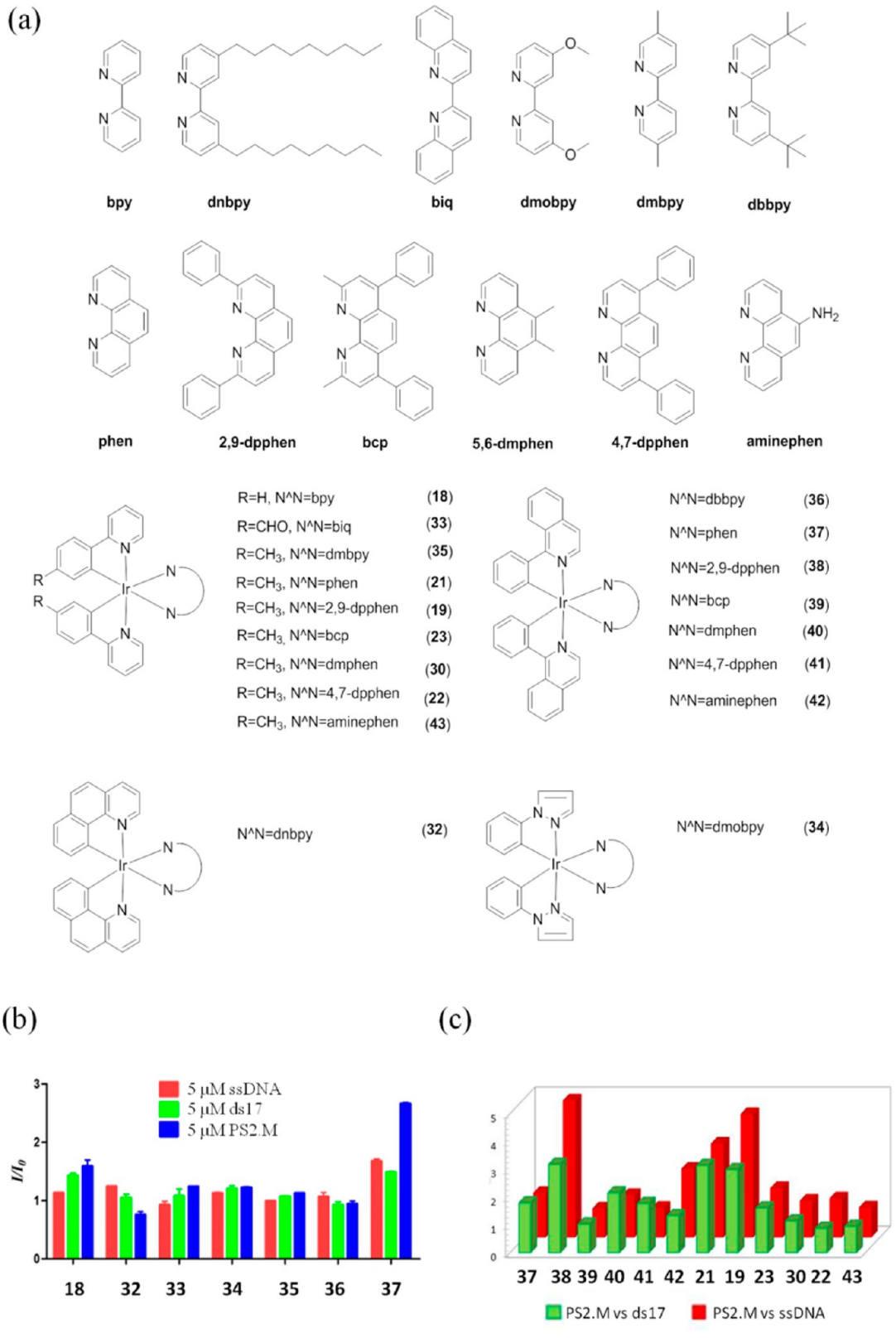

Figure 21. (a) Various iridium(III) complexes, (b) first round screening showing the luminescence response of complexes toward various DNAs, and (c) second round screening showing the luminescence enhancement selectivity ratio of complexes for G-quadruplex over dsDNA and ssDNA. Reproduced from ref 57 with permission. Copyright 2014 The Royal Society of Chemistry.

the G-tetrad for the other G-quadruplexes.[56] Furthermore, it is interesting to note that complex **24** carries the 2-chloro-1,10-phenanthroline (2-Clphen) N^N ligand and was the only halogenated complex screened in this study. This result therefore demonstrates again that the presence or absence of a single chloride ligand can have a significant influence on G-quadruplex selectivity. Finally, we also found that the luminescent intensity of **24** was dependent on the length of the G-quadruplex loops.

dx.doi.org/10.1021/ar500310z | *Acc. Chem. Res.* 2014, 47, 3614−3631

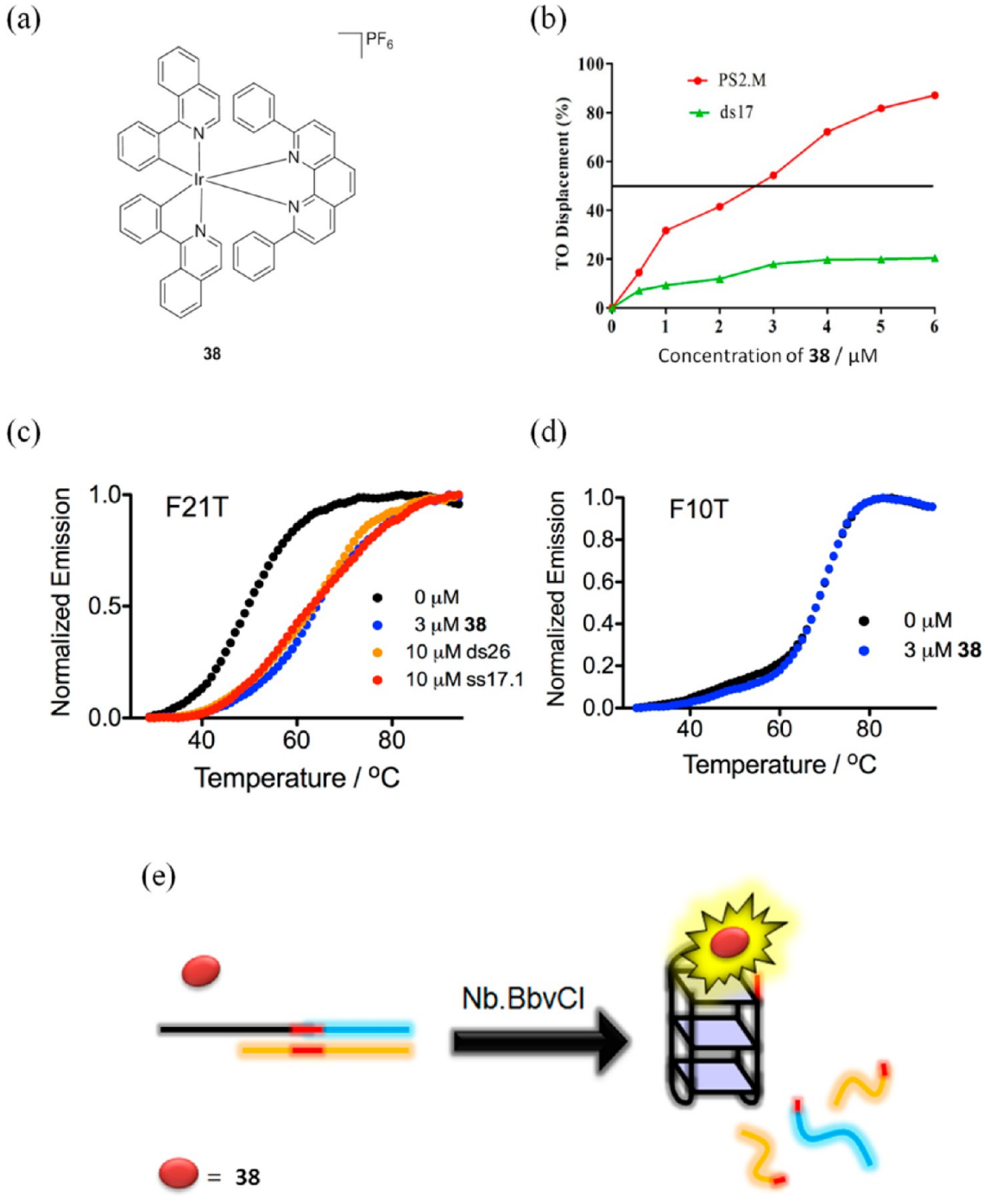

Figure 22. (a) Complex **38**, (b) G4-FID titration curves of DNA duplex ds17 and PS2.M G-quadruplex in the presence of increasing concentration of **38**, (c, d) melting profiles showing selectivity of **38**, and (e) G-quadruplex-based assay for nicking endonuclease activity. Reproduced from ref 57 with permission. Copyright 2014 The Royal Society of Chemistry.

In the Ag^+ ion assay, the addition of Ag^+ ions induces the formation of C−Ag^+−C mismatches in the cytosine-rich overhangs of the hairpin sequence (5′-$C_3TG_4AG_3TG_4AG_3TG_4A_2G_2CAGA_2G_2ATA_2C_2T_2C_4AC_3TC_4AC_3TC_4AC_3$-3′), allowing ExoIII to digest the 3′-terminus of the hybrid duplex. The liberated G-quadruplex-forming sequence then folds into a G-quadruplex structure that is subsequently recognized by **24**. As the Ag^+ ions are released from the hybrid duplex after digestion of the DNA, they could re-enter the cycle and trigger the next round of DNA cleavage, leading to an amplified luminescence response. This assay could detect down to 0.5 nM Ag^+ ions and was selective for Ag^+ ions over other metal ions such as K^+, Na^+, Ni^{2+}, Ca^{2+}, Zn^{2+}, Fe^{3+}, Mg^{2+}, and Pb^{2+} ions.

In a recent study, an initial screen of seven iridium(III) complexes **18** and **32**−**37** (Figure 21) bearing different N^N ligands found that only **37** (N^N = phen) displayed a selective response for G-quadruplex.[57] On the other hand, the other complexes were found to be nonselective for G-quadruplex. Based on the structure of **37**, a library of analogues containing analogues of phen as their N^N ligands was designed and synthesized. From the second round of screening, [$Ir(piq)_2$(2,9-dpphen)]PF_6 (**38**) was found to exhibit the highest selectivity for

dx.doi.org/10.1021/ar500310z | Acc. Chem. Res. 2014, 47, 3614−3631

Table 1. Biophysical Data of the G-Quadruplex Binding Affinity and Selectivity of Selected Iridium(III) Complexes

	G4-FID		FRET melting (F21T)		UV/vis titration		
complex	G4 sequence	DC_{50}, μM	ΔT, °C	[complex], μM	K_d, M^{-1} (G4)	K_d, M^{-1} (ss)	K_d, M^{-1} (ds)
5	ATP G4	>6	*a*	*a*	*a*	*a*	*a*
13	ATP G4	5	*a*	*a*	*a*	*a*	*a*
14	HTS	8.5	16	0.4	4.50×10^5	4.76×10^4	7.26×10^4
	Pu22	6.5					
	Pu27	5.5					
19	HTS	4.2	*a*	*a*	3.34×10^5	9.90×10^4	1.10×10^5
24	Pu27	2.5	8	5	1.29×10^5	4.49×10^4	4.02×10^4
38	PS2.M	2.5	7	3	*a*	*a*	*a*

[a]Not applicable.

the PS2.M G-quadruplex over ds17 (5′-$C_2AGT_2CGTAGTA_2C_3$-3′ and 5′-$G_3T_2ACTACGA_2CTG_2$-3′,) and ssDNA (5′-C_2AG-$T_2CGTAGTA_2C_3$-3′), with a maximal fold-change enhancement of 4.9 when bound to PS2.M. Further experiments using G4-FID and FRET-melting assays also confirmed **38** to be a G-quadruplex-selective probe (Figure 22). Like the G-quadruplex-selective complexes **13** and **19** described earlier, complex **38** also contains the piq (C^N) and 2,9-dpphen (N^N) ligands, respectively, indicating that the presence of those ligands are beneficial for G-quadruplex binding selectivity. Moreover, the selectivity of **38** for the PS2.M G-quadruplex was even greater than that exhibited by **19**, indicating that the piq C^N ligand may be superior to the ptpy C^N ligand of **19** for recognizing this specific G-quadruplex motif.

In the nicking endonuclease assay, an oligonucleotide (5′-$GTG_3TAG_3CG_3T_2G_2CTGAG_2TGA$-3′) containing a Nb.BbvCI cleavage site is partially hybridized with oligonucleotide 5′-$TCAC_2TCAGC_2A_2C_2$-3′. Treatment of the duplex substrate with Nb.BbvCI will result in cleavage of the Nb.BbvCI site, releasing the G-quadruplex-forming fragment that is recognized by **38**.

4. CONCLUSIONS AND FUTURE WORK

As described in this Account, our group has developed organometallic iridium(III)- and rhodium(III)-based compounds as molecularly targeted agents against specific pharmacological targets, including protein−protein interfaces that are typically considered to be difficult to target with small molecules. The next stage of analysis in our laboratory is to analyze the interactions between the metal complexes and the protein targets at the structural level, for example, by using X-ray crystallography or NMR spectroscopy in order to understand the binding mode of the metal complexes. This could even facilitate the rational design of metal complexes to specifically target critical amino acid residues within the binding site of enzymes or protein−protein interactions. The exploration of kinetically-inert group 9 complexes as inhibitors of protein−protein interactions has just begun and our view is that it will remain a fruitful field of investigation in the near future.

Our group has also harnessed the interesting photophysical behavior of iridium(III) complexes to develop luminescent label-free G-quadruplex-based detection platforms for various analytes. The assays rely on the "structure-switching" response of functional oligonucleotides in response to a target analyte, generating a G-quadruplex motif in solution that is recognized by the G-quadruplex-selective iridium(III) complexes with an enhanced luminescence response. As demonstrated by the examples in this Account, no single iridium(III) complex is the best for each sensing application. Instead, the optimal combination of metal complex and G-quadruplex sequence was determined empirically for each detection platform. Our preliminary findings have indicated that the size of the C^N and N^N ligands play an important role in G-quadruplex binding affinity, probably due to their influecnce on the end-stacking interactions with the terminal G-quartets. Moreover, we have shown that the incorporation of a single chloride moiety on the N^N ligand also can have a significant effect on G-quadruplex recognition. A summary of the biophysical data regarding the G-quadruplex binding affinity and selectivity of the iridium(III) complexes developed by our group is presented in Table 1.

Toward the future, a greater understanding between the structure of the iridium(III) complexes and their G-quadruplex binding specificities may allow these complexes to be tailored to target a specific G-quadruplex motif. In particular, complexes could be designed to bind to the more structurally heterogeneous groove and loop regions that are distinctive for each G-quadruplex topology, as a means of achieving superior selectivity. These studies can be supported by molecular modeling, X-ray crystallography, or NMR techniques to study the binding mode of the metal complexes to the G-quadruplex. With more selective iridium(III) complexes available, the sensitivity and specificity of G-quadruplex-based assays should be improved.

■ AUTHOR INFORMATION

Corresponding Authors

*E-mail: edmondma@hkbu.edu.hk.
*E-mail: duncanleung@umac.mo.

Funding

This work is supported by Hong Kong Baptist University (Grant FRG2/13-14/008), Centre for Cancer and Inflammation Research, School of Chinese Medicine (Grant CCIR-SCM, HKBU), the Health and Medical Research Fund (Grant HMRF/13121482), the Research Grants Council (Grants HKBU/201811, HKBU/204612, and HKBU/201913), the French National Research Agency/Research Grants Council Joint Research Scheme (Grant A-HKBU201/12), the State Key Laboratory of Synthetic Chemistry, the Science and Technology Development Fund, Macao SAR (Grant 103/2012/A3), and the University of Macau (Grants MYRG091(Y3-L2)-ICMS12-LCH, MYRG121(Y3-L2)-ICMS12-LCH, and MRG023/LCH/2013/ICMS).

Notes

The authors declare no competing financial interest.

Biographies

Dik-Lung Ma completed his Ph.D. in 2004 at the University of Hong Kong under the supervision of Prof. C.-M. Che. He spent the years

2005−2009 at the University of Hong Kong, the Hong Kong Polytechnic University, and the Scripps Research Institute with Prof. C.-M. Che, Prof. K.-Y. Wong, and Prof. R. Abagyan. In 2010, he was appointed Assistant Professor at the Hong Kong Baptist University. His research interests focus on luminescent sensing for biomolecules and metal ions, computer-aided drug discovery, and inorganic medicines.

Daniel Shiu-Hin Chan completed his B.Sc. degree in Chemistry at the University of New South Wales, Sydney, Australia. He is currently appointed as a Research Assistant at the Department of Chemistry at the Hong Kong Baptist University under the supervision of Dr. Dik-Lung Ma and Dr. Chung-Hang Leung.

Chung-Hang Leung completed his Ph.D. in 2002 at City University of Hong Kong. After completing a five year postdoctoral fellowship at the Department of Pharmacology, Yale University, he was appointed as Research Assistant Professor at the University of Hong Kong and then at the Hong Kong Baptist University. He is currently appointed as Associate Professor at the University of Macau. His research interests are in anticancer and anti-inflammatory drug discovery and molecular pharmacology.

REFERENCES

(1) Leung, C.-H.; Zhong, H.-J.; Chan, D. S.-H.; Ma, D.-L. Bioactive Iridium and Rhodium Complexes as Therapeutic Agents. *Coord. Chem. Rev.* **2013**, *257*, 1764−1776.

(2) Komor, A. C.; Barton, J. K. The Path for Metal Complexes to a DNA Target. *Chem. Commun.* **2013**, *49*, 3617−3630.

(3) Almodares, Z.; Lucas, S. J.; Crossley, B. D.; Basri, A. M.; Pask, C. M.; Hebden, A. J.; Phillips, R. M.; McGowan, P. C. Rhodium, Iridium, and Ruthenium Half-Sandwich Picolinamide Complexes as Anticancer Agents. *Inorg. Chem.* **2014**, *53*, 727−736.

(4) Zeglis, B. M.; Pierre, V. C.; Barton, J. K. Metallo-Intercalators and Metallo-Insertors. *Chem. Commun.* **2007**, 4565−4579.

(5) Katsaros, N.; Anagnostopoulou, A. Rhodium and its Compounds as Potential Agents in Cancer Treatment. *Crit. Rev. Oncol. Hematol.* **2002**, *42*, 297−308.

(6) Geldmacher, Y.; Oleszak, M.; Sheldrick, W. S. Rhodium(III) and Iridium(III) Complexes as Anticancer Agents. *Inorg. Chim. Acta* **2012**, *393*, 84−102.

(7) Liu, Z.; Sadler, P. J. Organoiridium Complexes: Anticancer Agents and Catalysts. *Acc. Chem. Res.* **2014**, *47*, 1174−1185.

(8) Dörr, M.; Meggers, E. Metal Complexes as Structural Templates for Targeting Proteins. *Curr. Opin. Chem. Biol.* **2014**, *19*, 76−81.

(9) You, Y.; Cho, S.; Nam, W. Cyclometalated Iridium(III) Complexes for Phosphorescence Sensing of Biological Metal Ions. *Inorg. Chem.* **2014**, *53*, 1804−1815.

(10) Yang, Y.; Zhao, Q.; Feng, W.; Li, F. Luminescent Chemodosimeters for Bioimaging. *Chem. Rev.* **2013**, *113*, 192−270.

(11) Zhao, Q.; Huang, C.; Li, F. Phosphorescent Heavy-Metal Complexes for Bioimaging. *Chem. Soc. Rev.* **2011**, *40*, 2508−2524.

(12) Fernandez-Moreira, V.; Thorp-Greenwood, F. L.; Coogan, M. P. Application of d^6 Transition Metal Complexes in Fluorescence Cell Imaging. *Chem. Commun.* **2010**, *46*, 186−202.

(13) You, Y.; Nam, W. Photofunctional Triplet Excited States of Cyclometalated Ir(III) Complexes: Beyond Electroluminescence. *Chem. Soc. Rev.* **2012**, *41*, 7061−7084.

(14) Chan, D. S.-H.; Fu, W.-C.; Wang, M.; Liu, L.-J.; Leung, C.-H.; Ma, D.-L. A Highly Selective and Non-Reaction Based Chemosensor for the Detection of Hg^{2+} Ions Using a Luminescent Iridium(III) Complex. *PLoS One* **2013**, *8*, No. e60114.

(15) Ma, D.-L.; He, H.-Z.; Chan, D. S.-H.; Wong, C.-Y.; Leung, C.-H. A Colorimetric and Luminescent Dual-Modal Assay for Cu(II) Ion Detection Using an Iridium(III) Complex. *PLoS One* **2014**, *9*, No. e99930.

(16) Ma, D.-L.; He, H.-Z.; Zhong, H.-J.; Lin, S.; Chan, D. S.-H.; Wang, L.; Lee, S. M.-Y.; Leung, C.-H.; Wong, C.-Y. Visualization of Zn^{2+} Ions in Live Zebrafish Using a Luminescent Iridium(III) Chemosensor. *ACS Appl. Mater. Interfaces* **2014**, *6*, 14008−14015.

(17) Lu, L.; He, H.-Z.; Zhong, H.-J.; Liu, L.-J.; Chan, D. S.-H.; Leung, C.-H.; Ma, D.-L. Luminescent Detection of Human Serum Albumin in Aqueous Solution Using a Cyclometallated Iridium(III) Complex. *Sens. Actuators, B* **2014**, *201*, 177−184.

(18) Jatiani, S. S.; Baker, S. J.; Silverman, L. R.; Reddy, E. P. Jak/STAT Pathways in Cytokine Signaling and Myeloproliferative Disorders: Approaches for Targeted Therapies. *Genes Cancer* **2010**, *1*, 979−93.

(19) Leung, C.-H.; Yang, H.; Ma, V. P.-Y.; Chan, D. S.-H.; Zhong, H.-J.; Li, Y.-W.; Fong, W.-F.; Ma, D.-L. Inhibition of Janus Kinase 2 by Cyclometalated Rhodium Complexes. *MedChemComm* **2012**, *3*, 696−698.

(20) Zhong, H.-J.; Yang, H.; Chan, D. S.-H.; Leung, C.-H.; Wang, H.-M.; Ma, D.-L. A Metal-Based Inhibitor of NEDD8-Activating Enzyme. *PLoS One* **2012**, *7*, No. e49574.

(21) Aktan, F. iNOS-Mediated Nitric Oxide Production and its Regulation. *Life Sci.* **2004**, *75*, 639−653.

(22) Liu, L.-J.; Lin, S.; Chan, D. S.-H.; Vong, C. T.; Hoi, P. M.; Wong, C.-Y.; Ma, D.-L.; Leung, C.-H. A Rhodium(III) Complex Inhibits LPS-Induced Nitric Oxide Production and Angiogenic Activity in Cellulo. *J. Inorg. Biochem.* **2014**, *140*, 23−28.

(23) Lievens, S.; Eyckerman, S.; Lemmens, I.; Tavernier, J. Large-Scale Protein Interactome Mapping: Strategies and Opportunities. *Expert Rev. Proteomics* **2010**, *7*, 679−690.

(24) Esposito, E.; Cuzzocrea, S. TNF-alpha as a Therapeutic Target in Inflammatory Diseases, Ischemia-Reperfusion Injury and Trauma. *Curr. Med. Chem.* **2009**, *16*, 3152−3167.

(25) Leung, C.-H.; Zhong, H.-J.; Yang, H.; Cheng, Z.; Chan, D. S.-H.; Ma, V. P.-Y.; Abagyan, R.; Wong, C.-Y.; Ma, D.-L. A Metal-Based Inhibitor of Tumor Necrosis Factor-α. *Angew. Chem., Int. Ed.* **2012**, *51*, 9010−9014.

(26) Miklossy, G.; Hilliard, T. S.; Turkson, J. Therapeutic Modulators of STAT Signalling for Human Diseases. *Nat. Rev. Drug Discovery* **2013**, *12*, 611−629.

(27) Ma, D.-L.; Liu, L.-J.; Leung, K.-H.; Chen, Y.-T.; Zhong, H.-J.; Chan, D. S.-H.; Wang, H.-M. D.; Leung, C.-H. Antagonizing STAT3 Dimerization with a Rhodium(III) Complex. *Angew. Chem., Int. Ed.* **2014**, *53*, 9178−9182.

(28) Zoncu, R.; Efeyan, A.; Sabatini, D. M. mTOR: From Growth Signal Integration to Cancer, Diabetes and Ageing. *Nat. Rev. Mol. Cell Biol.* **2011**, *12*, 21−35.

(29) Zhong, H.-J.; Leung, K.-H.; Liu, L.-J.; Lu, L.; Chan, D. S.-H.; Leung, C.-H.; Ma, D.-L. Antagonism of mTOR Activity by a Kinetically Inert Rhodium(III) Complex. *ChemPlusChem* **2014**, *79*, 508−511.

(30) Maksimoska, J.; Williams, D. S.; Atilla-Gokcumen, G. E.; Smalley, K. S. M.; Carroll, P. J.; Webster, R. D.; Filippakopoulos, P.; Knapp, S.; Herlyn, M.; Meggers, E. Similar Biological Activities of Two Isostructural Ruthenium and Osmium Complexes. *Chem.—Eur. J.* **2008**, *14*, 4816−4822.

(31) Ma, D.-L.; Wong, W.-L.; Chung, W.-H.; Chan, F.-Y.; So, P.-K.; Lai, T.-S.; Zhou, Z.-Y.; Leung, Y.-C.; Wong, K.-Y. A Highly Selective Luminescent Switch-On Probe for Histidine/Histidine-Rich Proteins and Its Application in Protein Staining. *Angew. Chem., Int. Ed.* **2008**, *120*, 3795−3799.

(32) Li, C.; Yu, M.; Sun, Y.; Wu, Y.; Huang, C.; Li, F. A Nonemissive Iridium(III) Complex That Specifically Lights-Up the Nuclei of Living Cells. *J. Am. Chem. Soc.* **2011**, *133*, 11231−11239.

(33) Man, B. Y.-W.; Chan, H.-M.; Leung, C.-H.; Chan, D. S.-H.; Bai, L.-P.; Jiang, Z.-H.; Li, H.-W.; Ma, D.-L. Group 9 metal-based inhibitors of β-amyloid (1−40) fibrillation as potential therapeutic agents for Alzheimer's disease. *Chem. Sci.* **2011**, *2*, 917−921.

(34) Georgiades, S. N.; Abd Karim, N. H.; Suntharalingam, K.; Vilar, R. Interaction of Metal Complexes with G-Quadruplex DNA. *Angew. Chem., Int. Ed.* **2010**, *49*, 4020−4034.

(35) Ambrus, A.; Chen, D.; Dai, J.; Bialis, T.; Jones, R. A.; Yang, D. Human Telomeric Sequence Forms a Hybrid-Type Intramolecular G-quadruplex Structure with Mixed Parallel/Antiparallel Strands in Potassium Solution. *Nucleic Acids Res.* **2006**, *34*, 2723−2735.

(36) He, H.-Z.; Chan, D. S.-H.; Leung, C.-H.; Ma, D.-L. G-quadruplexes for Luminescent Sensing and Logic Gates. *Nucleic Acids Res.* **2013**, *41*, 4345−4359.
(37) Du, Y.; Li, B.; Wang, E. "Fitting" Makes "Sensing" Simple: Label-Free Detection Strategies Based on Nucleic Acid Aptamers. *Acc. Chem. Res.* **2012**, *46*, 203−213.
(38) Lv, L.; Guo, Z.; Wang, J.; Wang, E. G-quadruplex as Signal Transducer for Biorecognition Events. *Curr. Pharm. Des.* **2012**, *18*, 2076−2095.
(39) Ma, D.-L.; Xu, T.; Chan, D. S.-H.; Man, B. Y.-W.; Fong, W.-F.; Leung, C.-H. A Highly Selective, Label-Free, Homogenous Luminescent Switch-on Probe for the Detection of Nanomolar Transcription Factor NF-kappaB. *Nucleic Acids Res.* **2011**, *39*, No. e67.
(40) He, H.-Z.; Leung, K.-H.; Yang, H.; Chan, D. S.-H.; Leung, C.-H.; Zhou, J.; Bourdoncle, A.; Mergny, J.-L.; Ma, D.-L. Label-free Detection of Sub-Nanomolar Lead(II) Ions in Aqueous Solution Using a Metal-Based Luminescent Switch-On Probe. *Biosens. Bioelectron.* **2013**, *41*, 871−874.
(41) He, H.-Z.; Chan, D. S.-H.; Leung, C.-H.; Ma, D.-L. A Highly Selective G-quadruplex-Based Luminescent Switch-On Probe for the Detection of Gene Deletion. *Chem. Commun.* **2012**, *48*, 9462−9464.
(42) Ma, D.-L.; Lin, S.; Leung, K.-H.; Zhong, H.-J.; Liu, L.-J.; Chan, D. S.-H.; Bourdoncle, A.; Mergny, J.-L.; Wang, H.-M. D.; Leung, C.-H. An Oligonucleotide-Based Label-Free Luminescent Switch-On Probe for RNA Detection Utilizing a G-quadruplex-Selective Iridium(III) Complex. *Nanoscale* **2014**, *6*, 8489−8494.
(43) Leung, K.-H.; Ma, V. P.-Y.; He, H.-Z.; Chan, D. S.-H.; Yang, H.; Leung, C.-H.; Ma, D.-L. A Highly Selective G-quadruplex-Based Luminescent Switch-On Probe for the Detection of Nanomolar Strontium(II) Ions in Sea Water. *RSC Adv.* **2012**, *2*, 8273−8276.
(44) Leung, K.-H.; He, H.-Z.; Ma, V. P.-Y.; Yang, H.; Chan, D. S.-H.; Leung, C.-H.; Ma, D.-L. A G-quadruplex-Selective Luminescent Switch-On Probe for the Detection of Sub-Nanomolar Human Neutrophil Elastase. *RSC Adv.* **2013**, *3*, 1656−1659.
(45) He, H.-Z.; Chan, W.-I.; Mak, T.-Y.; Liu, L.-J.; Wang, M.; Chan, D. S.-H.; Ma, D.-L.; Leung, C.-H. Detection of 3′ → 5′ Exonuclease Activity Using a Metal-Based Luminescent Switch-On Probe. *Methods* **2013**, *64*, 218−223.
(46) Leung, K.-H.; He, H.-Z.; Zhong, H.-J.; Lu, L.; Chan, D. S.-H.; Ma, D.-L.; Leung, C.-H. A Highly Sensitive G-quadruplex-Based Luminescent Switch-On Probe for the Detection of Polymerase 3′ to 5′ Proofreading Activity. *Methods* **2013**, *64*, 224−228.
(47) Leung, K.-H.; He, H.-Z.; Ma, V. P.-Y.; Chan, D. S.-H.; Leung, C.-H.; Ma, D.-L. A Luminescent G-Quadruplex Switch-on Probe for the Highly Selective and Tunable Detection of Cysteine and Glutathione. *Chem. Commun.* **2013**, *49*, 771−773.
(48) He, H.-Z.; Wang, M.; Chan, D. S.-H.; Leung, C.-H.; Qiu, J.-W.; Ma, D.-L. A Label-Free G-quadruplex-Based Luminescent Switch-On Assay for the Selective Detection of Histidine. *Methods* **2013**, *64*, 205−211.
(49) He, H.-Z.; Wang, M.; Chan, D. S.-H.; Leung, C.-H.; Lin, X.; Lin, J.-M.; Ma, D.-L. A Parallel G-Quadruplex-Selective Luminescent Probe for the Detection of Nanomolar Calcium(II) Ion. *Methods* **2013**, *64*, 212−217.
(50) Leung, K.-H.; Lu, L.; Wang, M.; Mak, T.-Y.; Chan, D. S.-H.; Tang, F.-K.; Leung, C.-H.; Kwan, H.-Y.; Yu, Z.; Ma, D.-L. A Label-Free Luminescent Switch-On Assay for ATP Using a G-Quadruplex-Selective Iridium(III) Complex. *PLoS One* **2013**, *8*, No. e77021.
(51) Leung, K.-H.; He, H.-Z.; Ma, V. P.-Y.; Zhong, H.-J.; Chan, D. S.-H.; Zhou, J.; Mergny, J.-L.; Leung, C.-H.; Ma, D.-L. Detection of Base Excision Repair Enzyme Activity Using a Luminescent G-quadruplex Selective Switch-On Probe. *Chem. Commun.* **2013**, *49*, 5630−5632.
(52) Leung, K.-H.; He, H.-Z.; Wang, W.; Zhong, H.-J.; Chan, D. S.-H.; Leung, C.-H.; Ma, D.-L. Label-Free Luminescent Switch-on Detection of Endonuclease IV Activity Using a G-Quadruplex-Selective Iridium(III) Complex. *ACS Appl. Mater. Interfaces* **2013**, *5*, 12249−12253.
(53) He, H.-Z.; Leung, K.-H.; Wang, W.; Chan, D. S.-H.; Leung, C.-H.; Ma, D.-L. Label-Free Luminescence Switch-On Detection of T4 Polynucleotide Kinase Activity Using a G-quadruplex-Selective Probe. *Chem. Commun.* **2014**, *50*, 5313−5315.
(54) Wang, M.; Leung, K.-H.; Lin, S.; Chan, D. S.-H.; Leung, C.-H.; Ma, D.-L. A G-Quadruplex-Based, Label-Free, Switch-on Luminescent Detection Assay for Ag^+ Ions Based on the Exonuclease III-Mediated Digestion of C-Ag^+-C DNA. *J. Mater. Chem. B* **2014**, *2*, 6467−6471.
(55) Monchaud, D.; Allain, C.; Bertrand, H.; Smargiasso, N.; Rosu, F.; Gabelica, V.; De Cian, A.; Mergny, J. L.; Teulade-Fichou, M. P. Ligands Playing Musical Chairs with G-Quadruplex DNA: A Rapid and Simple Displacement Assay for Identifying Selective G-Quadruplex Binders. *Biochimie* **2008**, *90*, 1207−1223.
(56) Hamon, F.; Largy, E.; Guédin-Beaurepaire, A.; Rouchon-Dagois, M.; Sidibe, A.; Monchaud, D.; Mergny, J.-L.; Riou, J.-F.; Nguyen, C.-H.; Teulade-Fichou, M.-P. An Acyclic Oligoheteroaryle That Discriminates Strongly between Diverse G-Quadruplex Topologies. *Angew. Chem., Int. Ed.* **2011**, *50*, 8745−8749.
(57) Lu, L.; Shiu-Hin Chan, D.; Kwong, D. W. J.; He, H.-Z.; Leung, C.-H.; Ma, D.-L. Detection of nicking endonuclease activity using a G-quadruplex-selective luminescent switch-on probe. *Chem. Sci.* **2014**, *5*, 4561−4568.